Energy & Buildings 286 (2023) 112971

Contents lists available at ScienceDirect

Energy & Buildings

journal homepage: www.elsevier.com/locate/enb

Climate change sensitive sizing and design for nearly zero-energy office building systems in Brussels

D. Amaripadath [a,*], R. Rahif [a], W. Zuo [b], M. Velickovic [c], C. Voglaire [c], S. Attia [a]

[a] Sustainable Building Design Lab, Department of UEE, Faculty of Applied Sciences, University of Liege, 4000 Liege, Belgium
[b] Department of Architectural Engineering, Pennsylvania State University, USA
[c] MK Engineering, 1050 Ixelles, Belgium

ARTICLE INFO

Article history:
Received 17 January 2023
Revised 21 February 2023
Accepted 6 March 2023
Available online 10 March 2023

Keywords:
Thermal discomfort
Overheating
Overcooling
Climate change resistivity
Energy use
Greenhouse gas emissions

ABSTRACT

As climate change continues, it is expected that the risk of overheating will rise in both new and existing buildings in mixed humid climate zones in Europe. This study introduced a novel climate change sensitive sizing and design approach for cooling and heating systems in nearly zero-energy office buildings in Brussels, Belgium, for different weather scenarios. This approach considered the long-term effects of climate change on building performance. The climate change effects were assessed using current and future climate data from the regional atmospheric model, MAR. To demonstrate the approach, a case study of a nearly zero-energy office building in Brussels was conducted. The reference building model was first calibrated using monthly energy use data from the year 2019 using ASHRAE Guideline 14. Then, the building was evaluated with different HVAC strategies and their performances were quantified. The results indicated an increase in overheating as high as 1.2 °C and cooling energy use as high as 13.5 kWh/m^2 and a decrease in overcooling as low as 0.3 °C and heating energy use as low as 10.9 kWh/m^2 in the reference building by the end of the century. In addition, due to climate change sensitive sizing and design approach coupled with optimal sizing, the reference building was climate change resistant towards the worst-case scenario by end of the century with up to 3.7 for climate change overheating resistivity and 20.2 for climate change overcooling resistivity. Finally, the paper provided recommendations for future practice and research based on the study findings.

© 2023 Elsevier B.V. All rights reserved.

1. Introduction

Climate change is widely acknowledged as one of the most serious threats of the 21st century, with severe and interconnected consequences for the environment, health, and economy [1,2]. Unusual weather events like heatwaves have become more common and severe around the world in the last decade, particularly during summer with temperatures ranging above 35 °C [2]. Parameters like precipitation, humidity, wind, and solar irradiance also change due to climate change [3]. The increasing rate of climate change causes long-term shifts in global temperatures and weather patterns either due to natural or anthropogenic sources. Anthropogenic climate change poses significant risks to society and the environment [4]. Fossil fuel combustion and industrial processes are the most common anthropogenic sources of climate change. Human-induced greenhouse gas (GHG) emissions are caused by energy use, industrial processes, agriculture, land-use change, forestry, etc. Furthermore, human-caused climate change will occur at a faster rate than natural one [5].

The average global surface temperature is expected to rise between 1 and 5.7 °C depending on the Shared Socioeconomic Pathway (SSP) scenario, as per Intergovernmental Panel on Climate Change (IPCC) Sixth Assessment Report (AR6) [6]. In addition to this, the urban heat island effect, which is defined as the relative

Abbreviations: ACD, Ambient Coolness Degree; AWD, Ambient Warmness Degree; ASHRAE, American Society of Heating, Refrigerating, and Air-Conditioning Engineers; CCOcR, Climate Change Overcooling Resistivity; CCOhR, Climate Change Overheating Resistivity; CDD, Cooling Degree Days; CIBSE, Charted Institution of Building Services Engineers; CV(RMSE), Coefficient of Variation of the Root-Mean-Square Error; DX, Direct Expansion; EEA, European Environment Agency; EN, European Norm; ESM, Earth System Model; EU, European Union; GCM, General Circulation Model; GHG, Greenhouse Gas; HDD, Heating Degree Days; HVAC, Heating, Ventilation, and Air Conditioning; IEA, International Energy Agency; IOcD, Indoor Overcooling Degree; IOhD, Indoor Overheating Degree; IPCC, Intergovernmental Panel on Climate Change; ISO, International Organization for Standardization; KPI, Key Performance Indicators; MAR, Modèle Atmosphérique Régional; NMBE, Normalized Mean Bias Error; nZEB, nearly Zero-Energy Buildings; PMV, Predicted Mean Vote; PPD, Predicted Percentage of Dissatisfied; SCORPION, Super COmputeR ProcessIng wOrkstatioN; SSP, Shared Socioeconomic Pathways; TMY, Typical Meteorological Year; VRF, Variable Refrigerant Flow.

* Corresponding author.
E-mail address: deepak.amaripadath@uliege.be (D. Amaripadath).

https://doi.org/10.1016/j.enbuild.2023.112971
0378-7788/© 2023 Elsevier B.V. All rights reserved.

atmospheric warmth of urban areas compared to the surrounding countryside, is expected to raise the temperatures by 5 °C to 10 °C in the cities [7,8]. The Urban Heat Island (UHI) is currently recognized in over 400 cities around the world [1,9]. Mitigation and adaptation to climate change are the two most important societal response options for reducing these risks. Mitigation in the context of climate change refers to limiting global climate change by reducing GHG emissions or improving their sinks. Adaptation refers to actions taken by vulnerable systems in response to actual or anticipated climate, to reduce climate change harm or maximize opportunities [4,6].

According to International Energy Agency (IEA), the building and construction sectors account for 36% of global final energy consumption and 40% of total direct and indirect CO_2 emissions [10,11]. Furthermore, IEA reports that energy demand in these sectors is still increasing due to improved access to energy in developing countries, increased ownership and use of energy-consuming devices, and rapid growth in the global building floor area, which is approaching 3% per year [10]. So, if a significant reduction in energy demand in buildings is required, the factors that contribute to energy consumption in buildings, such as Heating, Ventilation, and Air Conditioning (HVAC) must be identified and studied. There is a reciprocal connection between buildings and climate change because building energy use contributes to climate change and climate change generally leads to increased energy use [12]. Many studies have been conducted to investigate the impact of climate change on the energy performance of buildings [13–15]. Climate change has been found to increase the disparity between building heating and cooling demands, though the magnitude of this difference varies depending on the region and climatic zones [16,17].

The nearly Zero-Energy Buildings (nZEB) focus on potential climate change mitigation measures, such as reducing non-renewable energy consumption and thus CO_2 emissions. Usually, the emphasis is on how nZEBs reduce energy consumption and the costs of implementing energy-saving measures [18]. However, other important benefits are frequently overlooked. These are primarily concerned with indoor comfort and improved air quality, as well as the associated reduction in sick leave, health benefits, and increased productivity. Furthermore, lower burdens due to fluctuations in energy prices are expected, which will decrease the operation and maintenance costs [19]. These advantages improve the building quality and the user's well-being while also providing economic advantages, such as lower energy bills. To achieve an expected performance from the nZEBs, HVAC systems must be well designed by considering the variations in influential factors, such as outdoor weather conditions. Outdoor weather conditions are critical for estimating building thermal/electrical loads and renewable energy generation and thus influence the design of nZEB systems [20–22]. Extreme outdoor temperatures have a direct impact on a building's peak cooling and heating demand and, as a result, the size of the associated HVAC system [23].

Some relevant publications that examined the impact of climate change on thermal comfort, heating demand, cooling demand, and/or GHG emissions in European buildings are listed in Table 1. The studies on office buildings in Switzerland [24] revealed a 10.5 time increase in cooling energy demand in the future due to climate change. The study also suggests that the need for cooling systems in office buildings will become a crucial building design issue. The studies from Kolokotroni et al. [25] reiterate comparable results but also identify the urban heat island effect as a significant contributor to future cooling loads in addition to climate change. Studies from Cellura et al. [26] evaluated climate change effects on energy demands of office buildings in southern Europe and found that there would be an increase in the range of 51% to 120% in energy demands by the 2090s if the effects of climate change are not countered and limited. The results from Roetzel and Tsangrassoulis [27] indicate that thermal comfort optimization depends on building design, whereas energy consumption and GHG emissions depend on occupant behavior. The existing studies from Table 1 reveal that there will be a decrease in heating demand, an increase in cooling demand, and an increase in GHG emissions in the future. According to these findings, passive cooling alone will not be able to resist the heat stress in office buildings due to climate change and there is a growing need for active cooling in buildings to counter issues like overheating and ensure thermal comfort in the buildings.

From the review of existing literature, multiple knowledge gaps were identified. Firstly, the majority of the existing studies for commercial buildings in mixed humid climates (4A) in Europe are based on a unique assumption of HVAC systems, without specific information on the modeling, calibration, and/or sizing procedure. Secondly, there was a lack of studies that implements climate change sensitive sizing and design of HVAC systems along with optimal sizing factor. Thirdly, there was a scarcity of studies that implements time-integrated thermal discomfort analysis using multizonal thermal discomfort indices. Last but not the least, the existing literature from Table 1 [24–33] uses the Köppen-Geiger classification [34], which was dependent mainly based on ground coverage and precipitation, which makes it unfit for building performance analysis and bioclimatic design.

Due to the increasing effects of climate change, warmer winters, and hotter summers are foreseen in the future in mixed humid climates (4A) in Europe, adding to the building cooling loads in summers that will create extra stress on the existing electrical grids. Hence, it was important to study the changing behavior of the built environment and to better prepare to adapt to and mitigate the effects of future climate change. The purpose of this study was to increase the understanding of the thermal comfort and energy efficiency of commercial buildings while considering long-term climate change impacts and to use this understanding to support the transition at the regional and national levels in Belgium, and to a larger extent in Europe, which is in mixed humid climates (4A). Based on these observations, the research questions were formulated as follows:

How will indoor thermal comfort conditions vary due to climate change towards the end of the century?
How will buildings resist overheating and overcooling due to climate change towards the end of the century?
How will HVAC energy use and peak load demand shift due to climate change towards the end of the century?
How will buildings contribute to GHG emissions due to climate change towards the end of the century?

This paper sheds light on the importance of climate change sensitive thermal comfort evaluations and criteria being to be embedded in office building codes for policymakers. This has the potential to improve thermal comfort while also assisting the construction industry in its efforts to build climate change resistant office buildings. This paper also evaluates future HVAC energy use and GHG emissions, as well as how HVAC system selection may affect these parameters. The study gives an insight into future increases in electricity demand during summer due to an increase in building space cooling.

The novelty of the paper was based on several aspects:

1. The paper uses an innovative climate change sensitive sizing and design approach for HVAC systems in office buildings for various weather scenarios unlike the existing studies [35]. This approach has accounted for the long-term impacts of climate change on building performance. Here, the summer and winter design days for each weather scenario were calculated as per

Table 1
Summary of the recent studies on the impact of climate change on thermal comfort, heating demand, cooling demand, and GHG emissions in European office buildings.

Author(s)	Year	Building		ASHRAE 169 (or) Köppen-Geiger classification?	Study focus
		Type	Scale		
Frank [24]	2005	Commercial Residential	Building stock	Köppen-Geiger Zurich, Switzerland – Cfb	Heating demand Cooling demand
Kolokotroni et al. [25]	2012	Commercial	3-story office	Köppen-Geiger London, UK – Cfb	Thermal comfort Heating demand Cooling demand GHG emissions
Cellura et al. [26]	2018	Commercial	1-story office	Köppen-Geiger Multiple Southern European cities	Heating demand Cooling demand
Roetzel and Tsangrassoulis [27]	2012	Commercial	Office room	Köppen-Geiger Athens, Greece - Csa	Thermal comfort Heating demand Cooling demand GHG emissions
Boyano et al. [28]	2013	Commercial	3-story office	Köppen-Geiger Tallinn, Estonia – Dfb Madrid, Spain – Bsk London, UK – Cfb	Heating demand Cooling demand
Moreci et al. [29]	2016	Commercial	5-story office	Köppen-Geiger Multiple European cities	Heating demand
Sánchez-García et al. [30]	2020	Commercial	Simulation – shoebox Real-life – multi-story office	Köppen-Geiger Seville, Spain – Csa Madrid, Spain – Bsk Avila, Spain – Csb	Thermal comfort Heating demand Cooling demand
Hooyberghs et al. [31]	2017	Commercial	5-story office	Köppen-Geiger Antwerp, Belgium - Cfb Bilbao, Spain – Cfb London, UK – Cfb	Cooling demand
Masi et al. [32]	2021	Residential	Single-family house	Köppen-Geiger Benevento, Italy – Csa	Heating demand Cooling demand
Ascione et al. [33]	2022	Residential	nZEB of Benevento – Research lab	Köppen-Geiger Benevento, Italy – Csa	Heating demand Cooling demand

ISO 15927-2 [36] to ensure the resistivity of the building cooling and heating systems towards the long-term impacts of climate change.

2. The paper used an optimal sizing factor approach to account for the building's thermal inertia. This approach was building-specific, and the optimal value varies depending on the type and construction of the building. This strategy coupled with climate change sensitive sizing and design will ensure optimum indoor thermal comfort while ensuring maximum energy efficiency during long-term climate change. The calculations were realized using a parametric analysis with different weather scenarios as the variables and building unmet cooling and heating load hours as the output. The optimal sizing factor is defined as the factor at which the unmet load hours for cooling and heating systems are zero.
3. A time-integrated analysis was used in this paper to assess the degree of thermal discomfort in the reference building. Existing indices like Percentage out of Range (POR) from ISO 7730 [37] and implemented in [38], Exceedance Hours (Eh) from ASHRAE 55 [39] and implemented in [40,41], and Hours of Exceedance (HE) from CIBSE TM52 [42] and implemented in [43,44], measures the number of occupied hours that were outside the comfort limits. The results were then expressed as the percentage of the total occupied time. However, these indices do not measure the severity or the extent of discomfort in the building and predict comfort as a binary factor - comfortable vs. uncomfortable [45]. The time-integrated indices used in this study predict the degree and extent of discomfort and overheating in °C.
4. This paper uses climate classification as per ASHRAE 169 classification [46] in comparison to existing literature from Table 1 [24–33] that uses the Köppen-Geiger classification [34]. Köppen-Geiger classification in the existing literature was dependent mainly on the ground coverage and precipitation, which makes it unfit for building performance analysis and bioclimatic design. Whereas, ASHRAE 169 classification was based on Cooling Degree Days (CDD) and Heating Degree days (HDD), which were defined as the difference between the outdoor temperature and reference base temperature over a specified period and was more adapted to predict energy use in the buildings.

In this paper, ASHRAE 169 classification [46] was based on CDDs and HDDs. A region with more than 5400 HDDs with 18.3 °C as the basis, an average monthly outdoor temperature that falls below 7 °C during the winter, and annual precipitation of 50 cm, was considered a mixed humid climate (4A) according to this classification. The climatic zones of Europe and the study location according to the ASHRAE 169 classification [46] are shown in Fig. 1.

2. Methodology

An overview of the methodology used in this paper is shown in Fig. 2. The workflow of the study was as follows:

1. The innovative approaches that include climate change sensitive sizing and design using design day calculations, building specific optimal sizing factor calculation using parametric analysis, and key performance indicators (KPI) used in this study were universal and can be applied to any building.
2. The next stage was the selection of a case study to apply the above-mentioned approaches:

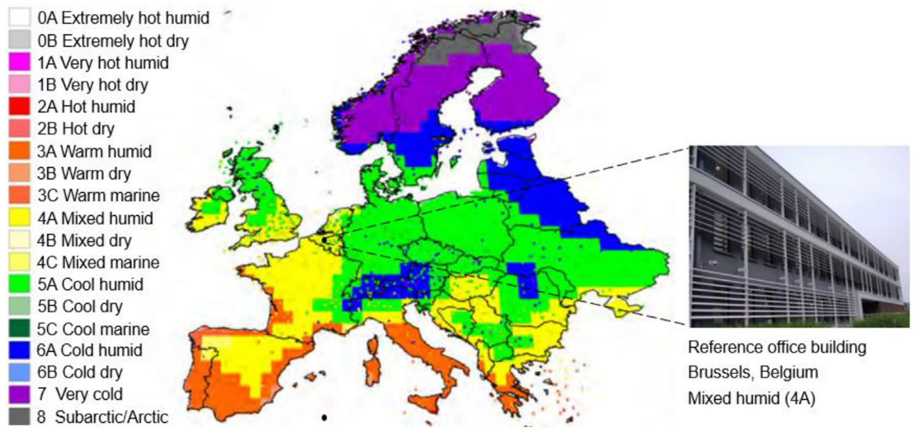

Fig. 1. European climate zones according to ASHRAE 169 climate classification [46].

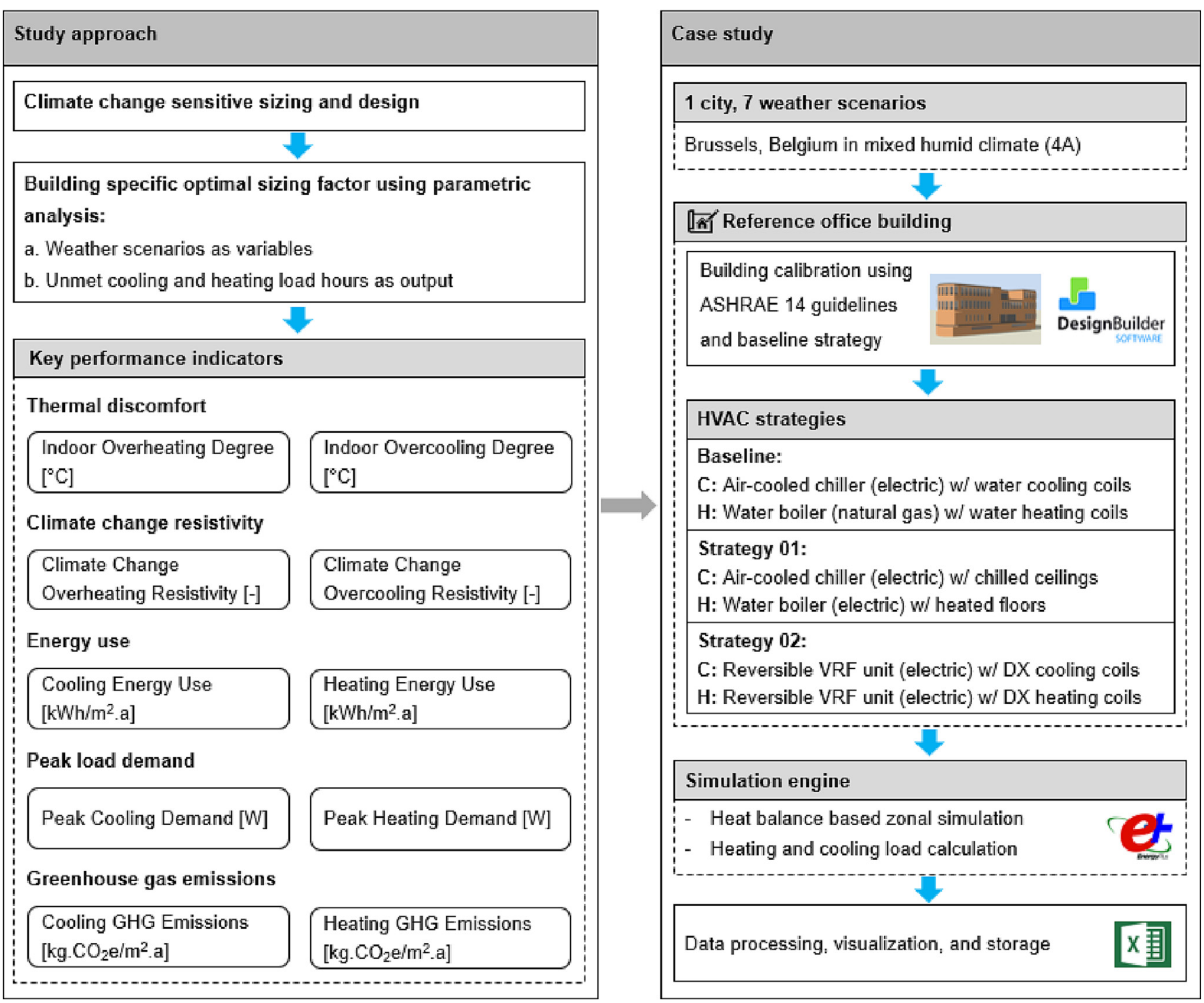

Fig. 2. Proposed workflow of the climate sensitive sizing and design approach.

a. A real office building with a baseline HVAC system of an air-cooled chiller (electric) with water cooling coils and a water boiler (natural gas) with water heating coils was identified near Brussels, Belgium.
b. The HVAC systems were sized and designed using a climate change sensitive approach. Optimal sizing factors were used for HVAC systems in this study through parametric analysis. Then, the building energy model was calibrated for the building envelope and HVAC baseline system.
c. The baseline was compared with 2 other HVAC retrofit strategies: (i) Strategy 01: an air-cooled chiller (electric) with chilled ceilings and a water boiler (electric) with heated floors, and (ii) Strategy 02: a reversible air-cooled VRF unit (electric) with DX cooling coils and DX heating coils for future scenarios.

3. The results of the case study were then quantified using key performance indicators for thermal discomfort, climate change resistivity, energy use, peak load demand, and GHG emissions. These KPIs were global and can be applied to different buildings and climate zones.

The building model was created using DesignBuilder v7.0.1 software, which is a comprehensive and user-friendly Graphical User Interface (GUI) for the EnergyPlus v9.6.0 simulation engine. The data processing, visualization, and storage were performed with Microsoft Excel. The CBE Clima Tool [47] was used to analyze the weather files. The formal analysis was carried out using a state-of-the-art workstation at the Sustainable Building Design Lab at the University of Liege, Super COmputeR ProcessIng wOrkstatioN (SCORPION) that uses a processor with 6 cores, 128 threads, and a 256 MB cache for the computing power and performance. This was in combination with 128 GB of Random Access Memory (RAM) and a graphics card of 24 GB that masters most scientific applications.

2.1. Study scope

The research was carried out on a representative case near Brussels, Belgium, which has a mixed humid climate (4A) according to the ASHRAE 169 classification [46]. The focus of the building design in such heating-dominated regions was primarily on heat preservation inside the building during winter. This was accomplished through highly insulated and airtight design concepts, which in turn obstruct heat dissipation during the summer season contributing to overheating phenomena in buildings. As a result, relying solely on passive cooling measures may make it difficult to prevent overheating issues in the future. It should be noted that the provisions, such as a reference building model, climate data, GHG emissions, and so on were required to understand and generalize the results to other mixed humid climates (4A). The building model was equipped with three different HVAC strategies to evaluate and compare the fitness of each strategy in varying weather scenarios in terms of time and SSPs.

2.2. Study approach

In this section, the study approach that can also be reproduced on other buildings, irrespective of the HVAC systems, building type, climate zones, etc. is discussed.

2.2.1. Climate change sensitive sizing and design

In this study, the HVAC sizing was adapted according to a climate change sensitive sizing and design approach, where the sizing was performed separately for each weather file for different periods and SSP scenarios. The design weather data was calculated using the methodology prescribed in ISO 15927-2 [36] with a focus on outdoor dry-bulb temperature [°C]. Hourly peak values of dry-bulb temperature were used for the design and sizing of cooling systems. This was briefly explained in [36]. The worst-case scenarios for both cooling and heating systems were identified for each weather scenario representing the current period for the 2010s and SSP2, SSP3, and SSP5 for the 2050s and 2090s. The climate data for different periods and SSPs calculated as per ISO 15927-2 [36] are listed in Table A.1 in Appendix A.

2.2.2. Building specific optimal sizing factor

To design an optimal indoor thermal comfort condition inside the building, the sizing factor for the cooling and heating systems should be calculated alongside a climate change sensitive sizing and design approach. This was done through parametric analysis of the building model with different HVAC strategies and weather scenarios. The optimal sizing factor was defined as the sizing factor at which the unmet load hours for cooling and heating systems are zero. The parametric analysis was performed with DesignBuilder software by choosing hourly weather data as the design variable and unmet load hours of cooling and heating systems as the outputs. Improper sizing of the HVAC systems can result in excessive noise, energy costs, indoor thermal discomfort, and bad indoor air quality [48]. Accurate and efficient sizing of HVAC systems will meet efficient performance while meeting the indoor thermal comfort and air quality expectations of the occupants [48]. The parametric analysis results for the building specific optimal sizing factor for HVAC systems are shown in Fig. 3. The unmet load hours for the cooling and heating system were zero for all weather scenarios for a sizing factor of one.

2.2.3. Key performance indicators

KPIs provide a critical and quantified measure of how the target parameter was performing under intended study conditions. The different KPIs used in this study are given below.

2.2.4. Time-integrated thermal discomfort

Thermal discomfort assessment in buildings requires the selection of appropriate indicators and underlying thermal comfort models. Thermal discomfort indicators can be symmetric in that they are overheating-specific and overcooling-specific, or asymmetric in that they are overheating-specific or overcooling-specific [49]. To estimate the overheating discomfort, an asymmetric index called the Indoor Overheating Degree (IOhD) [50] was chosen. In addition, another asymmetric index called the Indoor Overcooling Degree (IOcD) [35] was used in this study to quantify the overcooling discomfort separately from the overheating discomfort. The IOhD and IOcD are multizonal indices. The equations for calculating the IOhD and IOcD are given in (1) and (2) respectively.

$$\mathrm{IOhD} = \frac{\sum_{z=1}^{Z}\sum_{i=1}^{N_{occ}(z)}\left[\left(\mathrm{T}_{in,z,i} - \mathrm{T}_{comf,upper,z,i}\right)^{+} \times \mathrm{t}_{i,z}\right]}{\sum_{z=1}^{Z}\sum_{i=1}^{N_{occ}(z)}\mathrm{t}_{i,z}} \quad (1)$$

$$\mathrm{IOcD} = \frac{\sum_{z=1}^{Z}\sum_{i=1}^{N_{occ}(z)}\left[\left(\mathrm{T}_{comf,lower,z,i} - \mathrm{T}_{in,z,i}\right)^{+} \times \mathrm{t}_{i,z}\right]}{\sum_{z=1}^{Z}\sum_{i=1}^{N_{occ}(z)}\mathrm{t}_{i,z}} \quad (2)$$

where Z is the total conditioned zones in the building, i is the occupied hour counter, $N_{occ}(z)$ is the total number of zonal occupied hours in zone z, $\mathrm{T}_{in,z,i}$ is the indoor operative temperature in zone z at time step i in [°C], $T_{comf,upper,z,i}$ is the maximum comfort threshold in zone z at hour i in [°C], and $T_{comf,lower,z,i}$ is the minimum comfort threshold in zone z at hour i in [°C]. The $T_{comf,upper,z,i}$ and $T_{comf,lower,z,i}$ can be derived from the PMV/PPD or adaptive comfort models in the standards, such as EN 16798-1 [51], ISO 17772 [52],

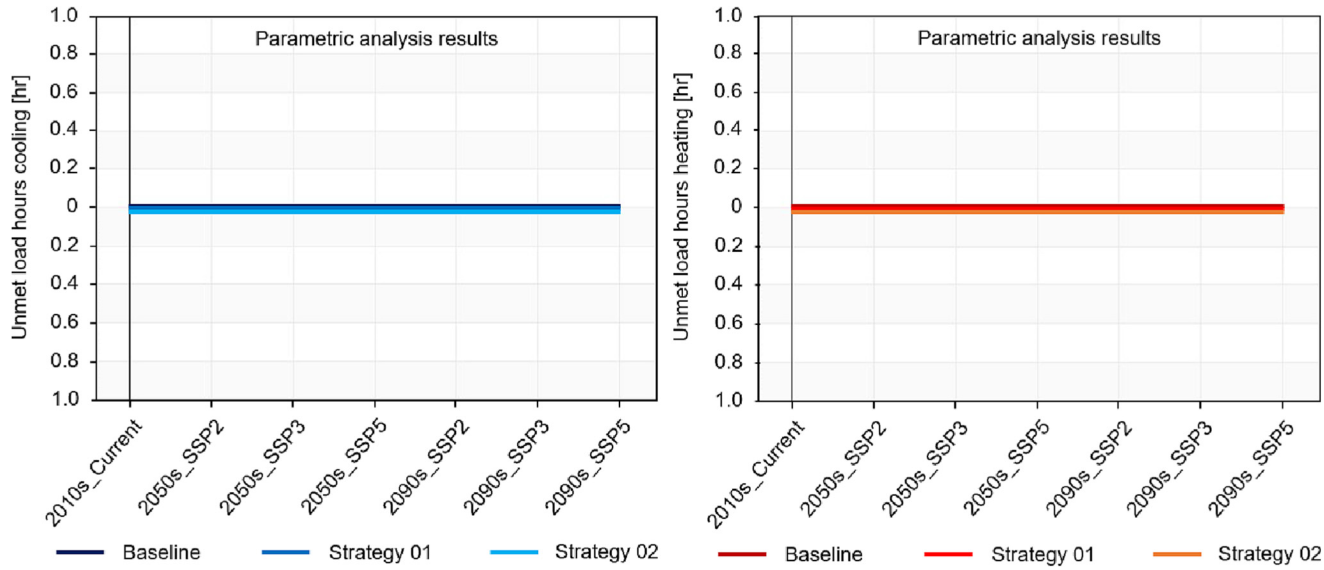

Fig. 3. Parametric analysis results for cooling and heating unmet hours of various HVAC strategies used in the reference nearly zero-energy building with an optimal sizing factor of 1.

ASHRAE 55 [39], CIBSE Guide A [53], etc. The comfort model used in this paper is based on EN 16798-1 category II for the PMV/PPD model, which is recommended for new buildings and renovations with active cooling systems [51]. The adaptive comfort model is not applicable here because the reference building is actively cooled during the occupied hours.

2.2.5. Climate change resistivity

Climate change resistivity is indicated through KPIs for overheating and overcooling resistivity. Climate Change Overheating Resistivity (CCOhR) [54] is shown in (3) and Climate Change Overcooling Resistivity (CCOcR) is shown in (4).

$$\frac{1}{CCOhR} = \frac{\sum_{Sc=1}^{Sc=M}(IOhD_{Sc} - \overline{IOhD}) \times (AWD_{Sc} - \overline{AWD})}{\sum_{Sc=1}^{Sc=M}(AWD_{Sc} - \overline{AWD})^2} \quad (3)$$

$$\frac{1}{CCOcR} = \frac{\sum_{Sc=1}^{Sc=M}(IOcD_{Sc} - \overline{IOcD}) \times (ACD_{Sc} - \overline{ACD})}{\sum_{Sc=1}^{Sc=M}(ACD_{Sc} - \overline{ACD})^2} \quad (4)$$

where Sc is the weather scenario counter, M is the total number of weather scenarios. $\overline{IOhD}$ and $\overline{AWD}$ are the averages of the total $IOhDs$ and $AWDs$. $CCOhR > 1$ means that the structure can withstand the increasing outdoor thermal stress caused by climate change, and $CCOhR < 1$ means that the structure is unable to withstand the increasing outdoor stress caused by climate change. $\overline{IOcD}$ and $\overline{ACD}$ are the averages of total $IOcDs$ and $ACDs$. $CCOcR > 1$ means that the structure can withstand the increasing outdoor thermal stress caused by climate change, and $CCOcR < 1$ means that the structure was unable to withstand the increasing outdoor stress caused by climate change. Both $CCOhR$ and $CCOcR$ are calculated for the current scenario and the worst mid-future and future scenario SSP5.

Ambient warmness Degree (AWD) and Ambient Coolness Degree (ACD) are listed in (5) and (6). AWD [°C] measures the severity of outdoor thermal conditions by averaging CDDs. ACD [°C] measures the severity of outdoor thermal conditions by averaging HDDs.

$$AWD = \frac{\sum_{i=1}^{N}\left[(T_{out,a,i} - T_b)^+ \times t_i\right]}{\sum_{i=1}^{N} t_i} \quad (5)$$

$$ACD = \frac{\sum_{i=1}^{N}\left[(T_b - T_{out,a,i})^+ \times t_i\right]}{\sum_{i=1}^{N} t_i} \quad (6)$$

2.2.6. Energy use and peak load demand

The building energy use was calculated for the cooling and heating systems in the building. Cooling energy use [kWh/m^2.a] is the total amount of annual energy used by the cooling systems with system fans for space cooling per square meter of the conditioned building spaces, whereas the peak cooling demand [W] is the energy used by the cooling systems with system fans to remove the amount of heat over an hour to maintain a comfortable room temperature during the hottest period during summer. The total amount of annual energy used by the heating systems with system fans for space heating per square meter of the conditioned building spaces was represented by heating energy use [kWh/m^2.a] whereas, the peak heating demand [W] was the energy used by the heating systems with system fans to add the amount of heat over an hour to maintain a comfortable room temperature during the coldest period during winter. The energy use was converted into primary energy use using a coefficient of 2.5 for electricity and 1 for natural gas as per the Belgian regulations [55,56].

2.2.7. GHG emissions

Cooling and heating GHG emissions were calculated separately in the paper to determine the impact of cooling and heating energy use on the environment. The emissions from the energy used for space cooling per square meter of the conditioned spaces including the cooling system and system fans were represented by cooling GHG emissions [kg.CO_2e/m^2.a]. The emissions from the energy used for space heating per square meter of the conditioned spaces including the heating system and system fans were represented by heating GHG emissions [kg.CO_2e/m^2.a]. The final energy use was converted from kWh to kg.CO_2e using Belgian emission coefficients of 0.270 kg.CO_2e/kWh for electricity and 0.181 kg.CO_2e/kWh for natural gas [57]. The GHG emissions are calculated to the current energy mix in Belgium, which is heavily dependent on non-renewable fossil fuels and nuclear energy. The GHG emissions will be reduced with increased integration of renewable sources in the Belgian energy mix.

2.3. Case study

In this section, the case study specifications like the climate data, building model, building calibration, and HVAC strategies are discussed.

2.3.1. Climate data

Acquiring reliable current and future climate data is critical in any climate change study and this determines the quality of the study [58]. The climate data used in this paper were based on the outputs of the General Circulation Model (GCM). Due to their high spatial and temporal resolutions, GCMs were used to estimate climate projections but were not directly applicable to building simulations. It was necessary to use downscaling techniques to convert them into compatible climate data through statistical or dynamic methods. The regional climate model Modele Atmospherique Regional (MAR) in version 3.11.14 [59] was used for this purpose, which was a dynamic method resulting in physically consistent climate parameters and extreme weather events and specially adapted and widely validated for Belgium [60–62].

A three-dimensional atmospheric model was coupled to a one-dimensional transfer scheme between the atmosphere, vegetation, and surface used to derive MAR [63]. Two different methods were used to calculate the climate data used in this paper: (i) Between 1980 and 2014, MAR was forced every six hours in its lateral boundaries by reanalysis ERA5 [64] assimilated by various sources of observations, e.g., in-situ weather stations, radar data, and satellites. This was considered a reconstruction of the observed climate data, and (ii) The Earth System Model (ESM) BCC-CSM2-MR, which approximately follows the mean temperature of all ESMs SSP5 to SSP8.5 over Belgium until the year 2100 from the Sixth Coupled Model Intercomparison Project (CMIP6) was used to force MAR every six hours, representing the mean evolution of climate parameters between 1980 and 2100 [65]. The ESM forced MAR was then validated by comparing it to MAR-ERA5 simulations to see if it could be used to generate future climate data [66].

The ESM forced MAR was then validated by comparing it to the MAR-ERA5 simulations to verify whether it can be used to create future climate data [66]. Future ESMs were built on SSPs, which were scenarios of worldwide socioeconomic evolution by the year 2100. These SSPs were used to calculate the GHG emissions associated with various climate strategies. The future climate data used in this paper comprise three SSPs: (i) SSP2 - medium challenges to mitigation and adaptation with an estimated 1.8 °C increase in global warming by 2100, (ii) SSP3 - high challenges to mitigation and adaptation with an estimated 3.6 °C increase in global warming by 2100, and (iii) SSP5 - high challenges to mitigation and low challenges to adaptation with an estimated 4.4 °C increase in global warming by 2100 [67,68].

After obtaining the MAR-BCC-CSM2-MR results, the Typical Meteorological Year (TMY) was constructed over 20 years for three different periods: 2001 to 2020, hereafter 2010s, 2041 to 2060, hereafter 2050s, and 2081 to 2100, hereafter 2090s. TMYs were synthetic years formed on an hourly basis by typical representative months chosen from the target period, e.g., from the target period like 2001 to 2020, and representative months like January 2001, February 2012, and so on. Using Finkelstein-Shafer statistics, the typical months were chosen by comparing the monthly long-term distribution of the available modeled or observed data for a minimum of ten years. The TMYs were created using the protocol from ISO 15927-4 [69] for Brussels in Belgium. The method includes reconstituting the months of the year by the most typical month for Brussels during the considered period. The comparison is mainly based on dry bulb temperature at 2 m above ground level. This variable was considered since it influences the comfort in the buildings. Therefore, the TMYs used in this study were generated as per dry bulb temperature 2 m above the ground level. The main steps followed to find typical months for each parameter are as follows [66]:

1. Converting an hourly file into a daily file: The daily mean of the climate variable is computed from all the hourly data from all the same calendar months available within the given timeframe.
2. Identifying the typical month: The 50th percentile of the climate variable is calculated for each calendar month across the timeframe to determine the month which is the most similar to the 50th percentile of this variable.
3. Extraction of typical month hourly data: Lastly, the hourly weather values for this typical month are saved in the file for the typical year.

For this study, TMY files were produced for periods of 2010s_Current, 2050s_Midfuture, and 2à90s_Future, along with various SSP scenarios like SSP2, SSP3, and SSP5. The TMY files from MAR are in CSV format and are comma-separated. The files were converted to epw format before using them with the DesignBuilder. The structure of the weather file contains hourly data of the weather variables listed in Table 2. The peak cooling load in the building is affected mainly by TMY files based on dry-bulb temperature, measured 2 m above the ground level [66].

The weather summary of TMY files in terms of Heating Degree Days (HDD), Cooling Degree Days (CDD), annual average air temperature, annual hottest air temperature, coldest air temperature, and cumulative horizontal solar radiation for each weather scenario was calculated using CBE Clima Tool [47] is shown in Fig. 4.

The $HDD_{10\,°C}$ values fall from the 2050s to 2090s and from SSP2 to SSP5, whereas the $CDD_{18°C}$ increases from 2050s to 2090s and from SSP2 to SSP5. The average decrease of $HDD_{10\,°C}$ from SSP2 to SSP5 is 24% by 2050s and 42% by 2090s. The average increase of $CDD_{18\,°C}$ from SSP2 to SSP5 was 21% by the 2050s and 60% by the 2090s. The increase in average annual air temperature for different scenarios is as follows: (i) for SSP2 scenarios, the average annual air temperature rises by 1.2 °C by 2050s and 1.7 °C by 2090s, (ii) for SSP3 scenarios, the average annual air temperature rises by 1.4 °C by 2050s and 2.7 °C by 2090s, and (iii) for SSP5 scenarios, the average annual air temperature rises by 1.7 °C by 2050s and 3.3 °C by 2090s. Among all 7 TMY files evaluated, the 2090s_SSP3 scenario gives the annual hottest air temperature of 34.7 °C, and the 2010s_Current gives the annual coldest air temperature of −6.4 °C. The annual cumulative horizontal solar radiation was at the lowest for the 2010s_Current at 1024.8 kWh/m^2 and highest for the midfuture scenario 2050s_SSP5 at 1132.6 kWh/m^2.

Table 2
Weather variables, measured levels, and units of the TMYs used in this study [66].

Weather variable	Level	Unit
Dry bulb temperature	2 m above ground level	°C
Relative humidity	2 m above ground level	%
Global horizontal radiation	Ground (horizontal surface)	W/m^2
Diffuse solar radiation	Ground (horizontal surface)	W/m^2
Direct normal radiation	Ground (horizontal surface)	W/m^2
Wind speed	10 m above ground level	m/s
Wind direction	10 m above ground level	North degrees
Dew point temperature	2 m above ground level	°C
Atmospheric pressure	Ground	Pa
Cloudiness	All troposphere	Tenths
Sky temperature	All troposphere	K
Specific humidity	2 m above ground level	–
Precipitation	Ground	mm

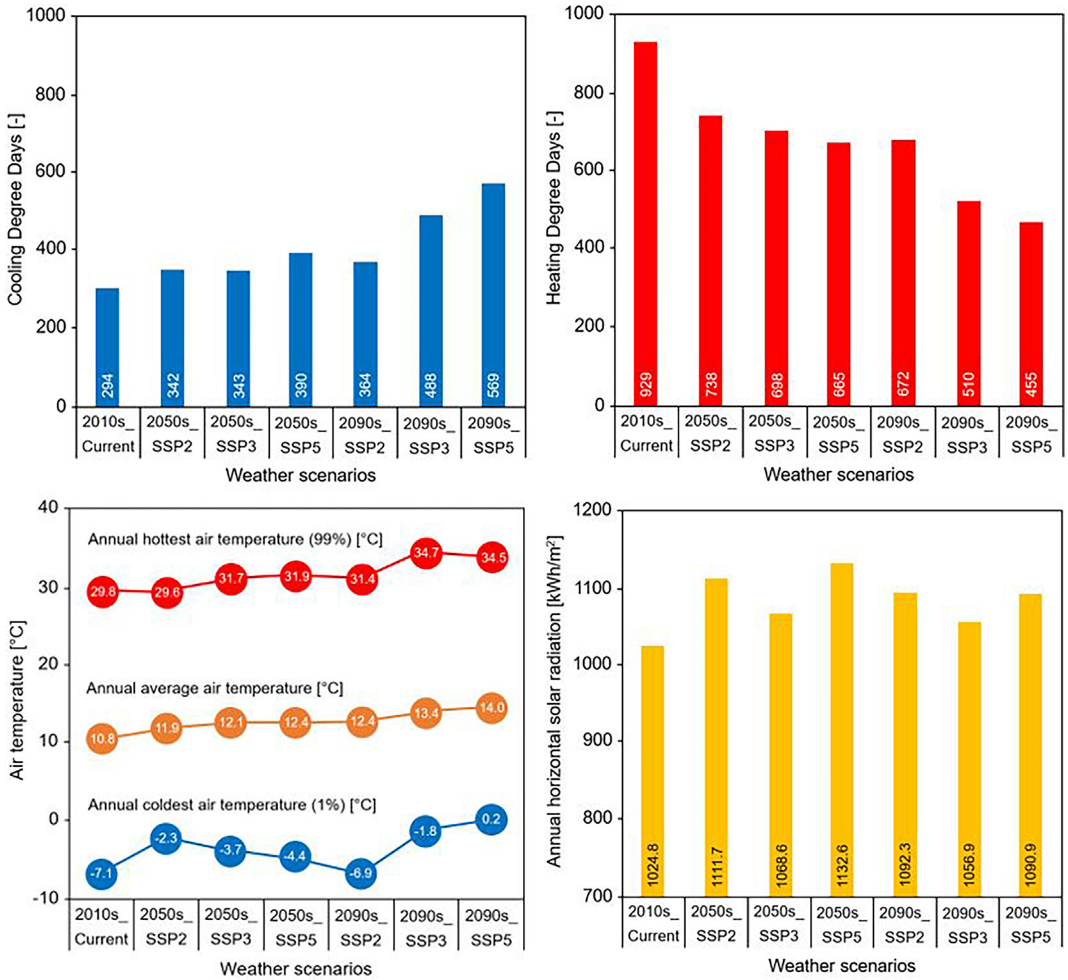

Fig. 4. Weather summary for current and future TMYs for different SSP scenarios.

2.3.2. Building model

The reference building was located near Brussels, Belgium, at a latitude and longitude of 50° 40′ 04.7″ N and 4° 33″ 39.7″ E, and an elevation of 112 m. The nZEB has three floors and a basement parking lot. It has a multipurpose hall, office rooms, meeting rooms, and other amenities. The structure was compact and had fixed solar protection. The DesignBuilder interface was used to create the model. The levels of the building were modeled using a multizonal approach to better perceive the potential overheating issues and to better assess the model's cooling needs. All constructive nodes have been identified according to the Performance Energetique des Batiments (PEB) Brussels [70]. The building can accommodate a maximum of 357 people, with 168 people in the multipurpose hall and 189 people in other conditioned spaces like office rooms, meeting rooms, and cafeterias. The building is not surrounded by any adjacent buildings.

In Belgium, the federal government has established the legal zero energy concept as requiring adherence to passive house standards. On a regional level, the application and calculation are different [71,72]. Local governments generally follow the concept that demand should be as low as possible before exploring renewable energy sources. The PHPP calculation model for non-residential buildings in Belgium stipulates the following requirements [71,72]:

1. The total energy demand for space heating and cooling must be less than or equal to 15 kWh/m^2 of conditioned floor area.
2. The total primary energy use for all appliances, domestic hot water, and space heating and cooling is limited to a compactness formula as given below:

$$E_{PE} = [90 - 2.5 \times C] \tag{7}$$

where C is compactness defined as the ratio between the building volume and the envelope surface area.

3. During the pressurization tests, according to the EN 13829 [73] norm with a pressure difference of 50 Pascal between indoors and outdoors, the air loss should be less than or equal to 60% of the volume of the house per hour, i.e., n50 $\leq$ 0.6/h.
4. Comfort can be calculated using dynamic simulations and using methodologies listed in EN 16798-2 [74], such as Percentage Outside the Range, Degree Hours, or PPD-weighted criteria.

The cooling loads from these coils were added together to calculate the net cooling requirement for the entire building. The heating was modeled individually, and these individual heat emitters were connected to a gas boiler. Ventilation was modeled for each type of zone occupancy like office rooms, cafeterias, forums, etc. The reference building was a heavy concrete structure, with high thermal inertia. The reference building has high airtightness and insulation values. Hence, it was also important to calculate the optimal sizing factor at which the unmet cooling and heating load hours were zero using parametric analysis alongside a climate change sensitive approach with respect to various weather scenarios for desirable indoor thermal comfort conditions.

A detailed list of the building characteristics is added in Table B.1. in Appendix B. The building composition is as follows [75]:

- The ground floor has four layers and was made of urea formaldehyde foam (0.1327 m), cast concrete (0.1 m), floor screed (0.07 m), and timber flooring (0.03 m) from the outer to the inner layer.
- The internal floors were made of dense concrete slabs (0.1 m).
- The external roof has four layers and was made of asphalt (0.01 m), MW glass wool rolls (0.4 m), air gap (0.2 m), and plasterboard (0.013 m) from the outer to the inner layer.
- The external walls have four layers and were made of Brickwork (0.1 m), XPS extruded polystyrene (0.0785 m), concrete block (0.1 m), and Gypsum plastering (0.013 m) from the outer to the inner layer.

The building model is shown in Fig. 5.

2.3.3. Building calibration

Energy simulation calibration should be performed after the building has been fully operational for some time, usually about a year, gathering the actual energy used by the real building and then adjusting energy model inputs, so that the simulation output was close approximate to the real value [76]. The uncertainties during calibration usually arise from abnormal building operations [76] and complex interactions between different building systems [77]. The mathematical measurements concerning building calibration were addressed in ASHRAE Guideline 14 [78]. According to these guidelines, the simulation model shall have a Normalized Mean Bias Error (NMBE) of ±5% and a Coefficient of Variation of the Root-Mean-Square Error (CV(RMSE)) of 15% relative to the monthly calibration data with at least 12 monthly utility data spanning for one year [78]. The building model was calibrated by adjusting the model inputs and approximating simulation output with monthly observed data from the real building for the year 2019 [79]. The NMBE [%] and CV(RMSE) [%] were 2.1% and 14.2% for electricity consumption and 2.1% and 12.8% for natural gas con-

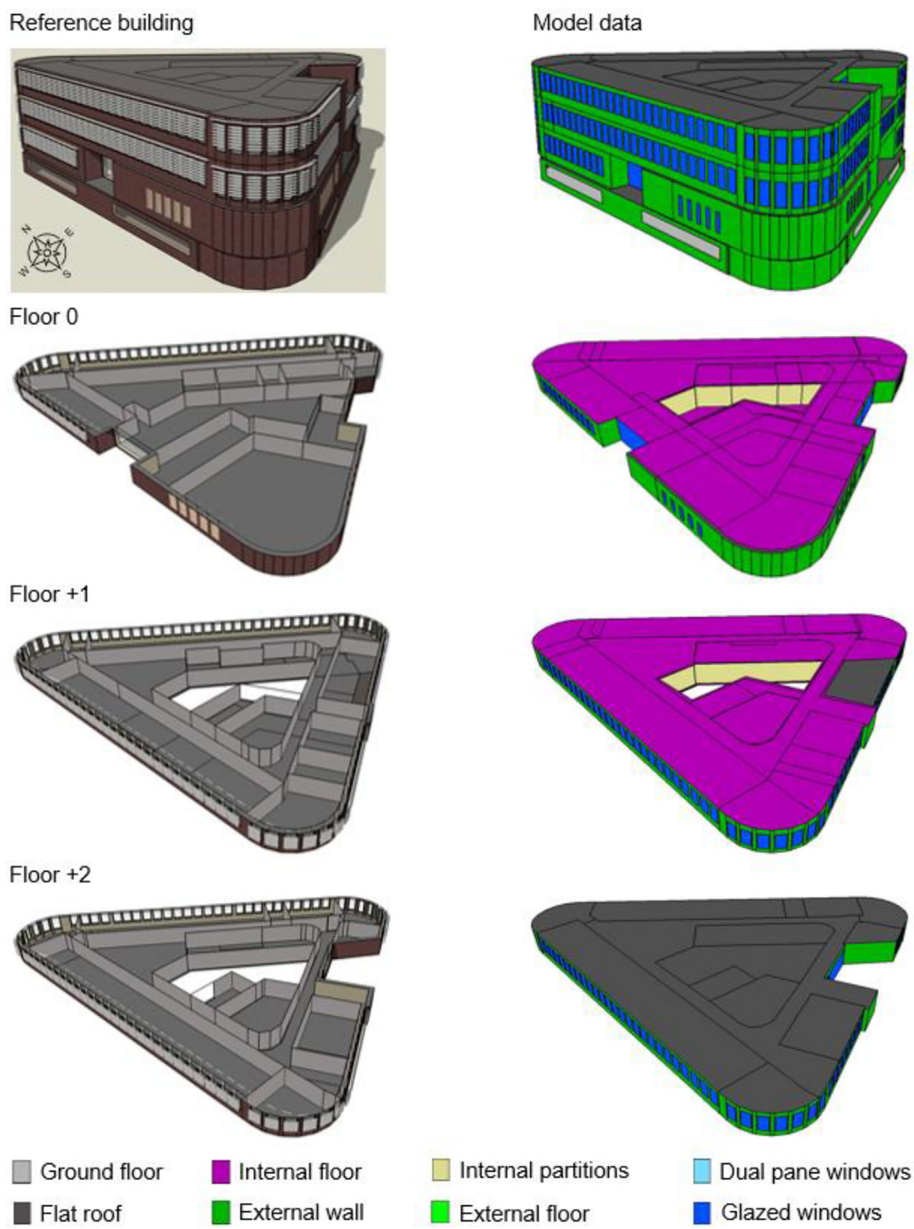

Fig. 5. Reference nearly zero-energy office building plans with geographic orientation.

sumption. These results are listed in Table C.1 in Appendix C. The real and calibrated model energy use is shown in Fig. C.1 in Fig. C.

2.3.4. HVAC strategies

The Baseline HVAC strategy used in this study was an air-cooled chiller (electric) with water cooling coils and a water boiler (gas) with water heating coils. The cooling system uses an air stream to transfer heat from the processed water using an evaporator in the chiller. The heating system operates by heating water using the gas boiler and then circulating it through the building. The hot water plant loop module in DesignBuilder was used to model the gas-fired water boiler. The baseline strategy is shown in Fig. 6. The airflow rates presented in Fig. 6 were obtained from the existing values in the reference building.

The first test HVAC strategy, Strategy 01 used in this study was an air-cooled chiller (electric) with chilled ceilings and a water boiler (electric) with heated floors. The system used an electric chiller and boiler with radiant cooling and heating panels for this study. A water-based radiant cooling and heating system are one in which the water acts as a medium for energy distribution, carrying the heat, and radiation accounts for more than half of the heat exchange with the conditioned space [80–82]. The control strategies like schedules were adopted based on modulated and continuous night operation for eight hours [82] and setpoint temperatures were selected based on a case study on an office building from Stuttgart, Germany, which was located in the same climate zone as Brussels, Belgium [83]. This HVAC strategy is shown in Fig. 7. The airflow rates presented in Fig. 7 were calculated as recommended by EN 16798-1 [51].

The second test HVAC strategy, Strategy 02 used in this study was a reversible VRF unit (electric) with DX cooling coils and DX heating coils. In addition to providing distributed, temperature-controlled room units, VRF can simultaneously shift heating and cooling around the building, by utilizing reversible heat pump technology [84,85]. The rated COP value for cooling and heating for VRF systems was defined in DesignBuilder. The minimum and maximum temperature values, thresholds below and above which the cooling and heating system will be disabled can be also defined. These temperature limits can be either defined as dry bulb temperature or wet bulb temperature for the heating system, whereas only dry-bulb temperature for the cooling system. Here the cooling and heating capacity ratio boundary curves define the refrigerant temperature to the outdoor air temperature and are shown in Fig. D.1 in Appendix D. In this model, we have used default values within DesignBuilder as the temperature limits that were lower and higher than the worst-case scenarios of each weather file, which was available in DesignBuilder. This HVAC strategy is shown in Fig. 8. The airflow rates presented in Fig. 8 were calculated as recommended by EN 16798-1 [51].

With upcoming natural gas legislation packages from the European Commission aiming to steer away from fossil fuels like natural gas and more towards sustainable energy sources [86], a transition of HVAC fuel from natural gas to electricity, for building heating purposes was adopted for strategies Strategy 01 and Strategy 02. Hence the HVAC strategies except Baseline uses electricity to heat the building. These HVAC strategies were some of the common technologies that were used for cooling and heating purposes in office buildings [87]. The model characteristics and assumptions of different HVAC strategies that were evaluated are listed in Table B.2 in Appendix B.

3. Results

This study was carried out by analyzing the effects of climate change on indoor thermal comfort, climate change resistivity, energy performance, and GHG emissions in a reference office building in Brussels, Belgium. The study results were shared in the following sections. The results of this study provide insights into the design and performance of the following HVAC strategies in the reference building: (i) Baseline: air-cooled chiller (electric) with water cooling coils and water boiler (gas) with water heating coils, (ii) Strategy 01: air-cooled chiller (electric) with chilled ceilings and water boiler (electric) with heated floors, and (iii) Strategy

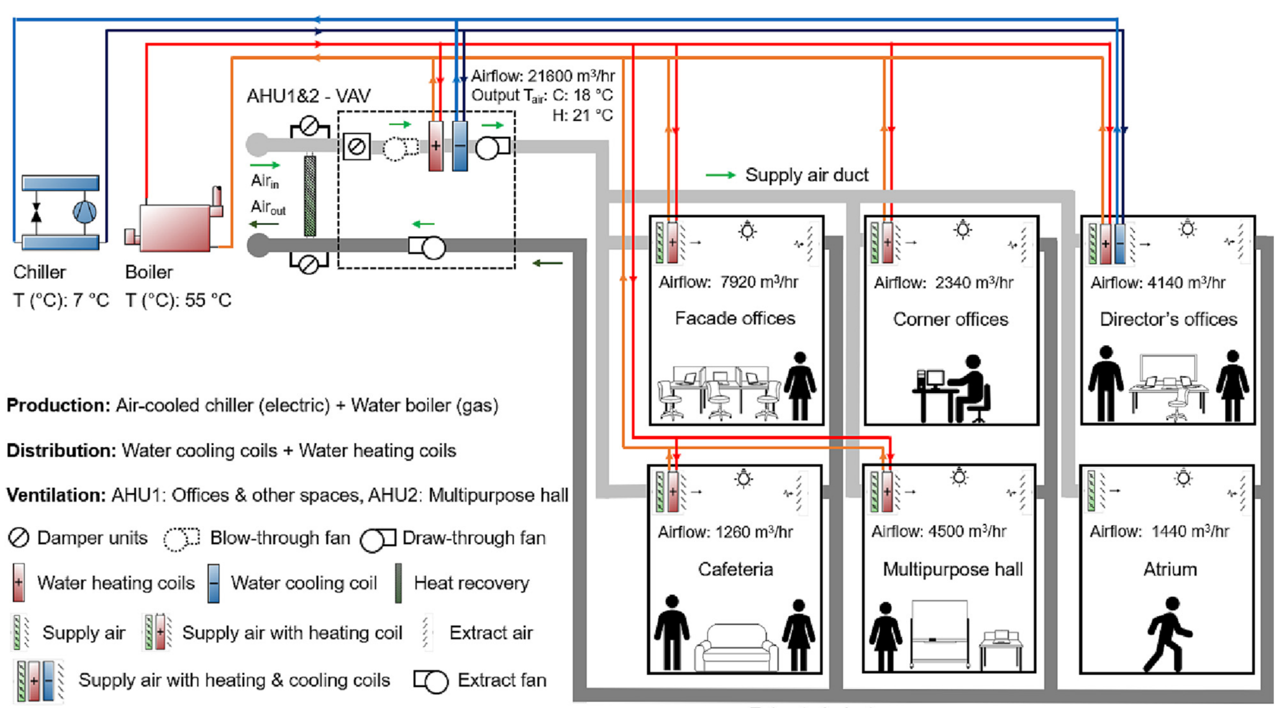

Fig. 6. Baseline: air-cooled chiller (electric) with water cooling coils and water boiler (gas) with water heating coils.

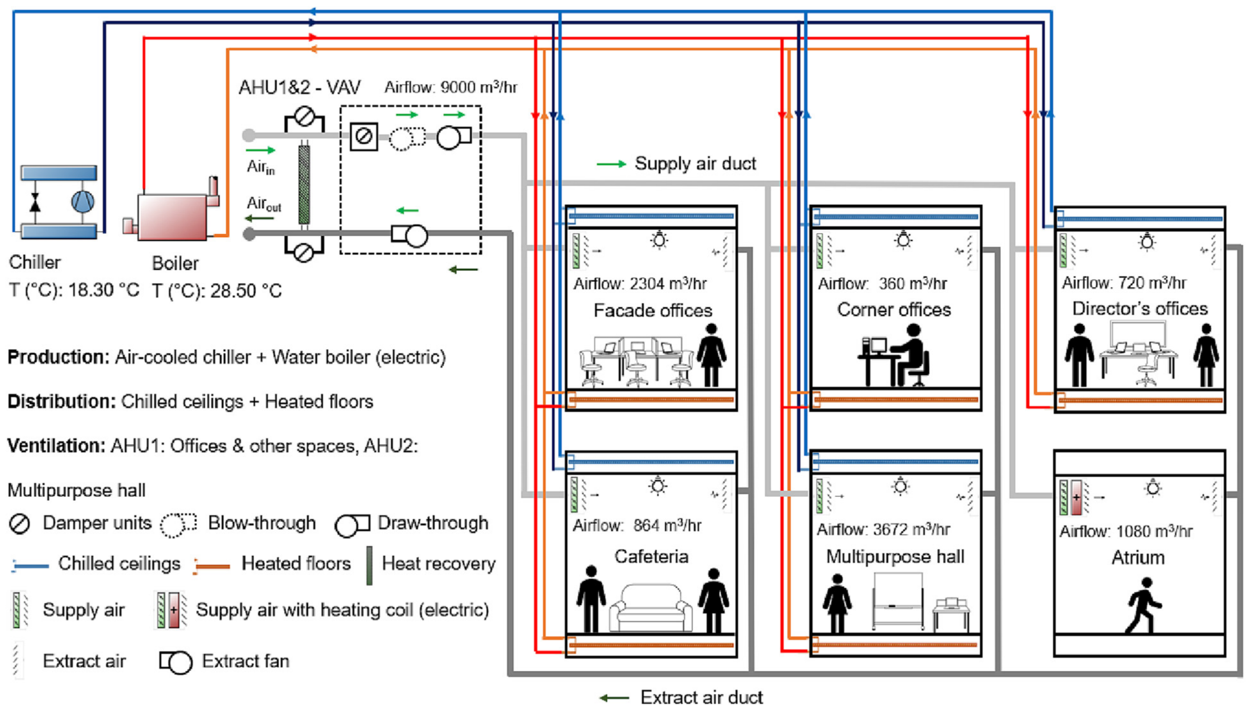

Fig. 7. Strategy 01: air-cooled chiller (electric) with chilled ceilings and water boiler (electric) with heated floors.

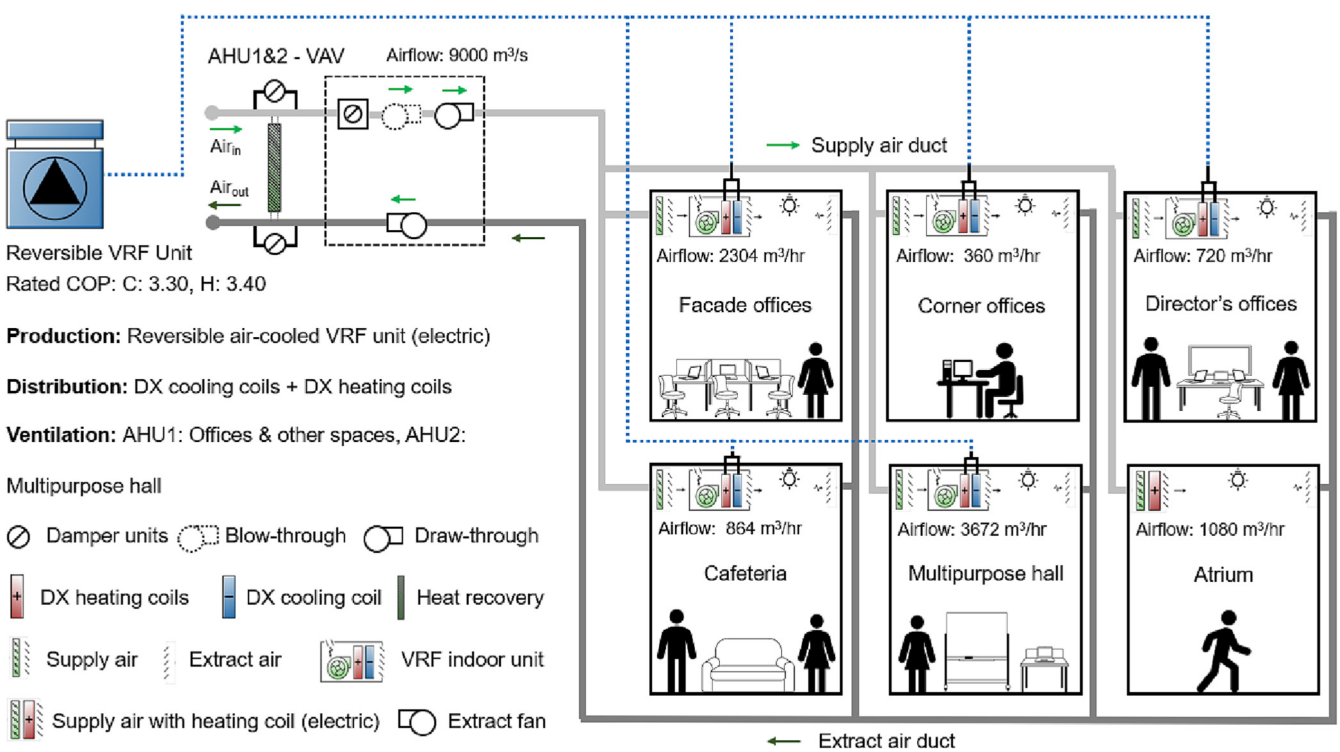

Fig. 8. Strategy 02: reversible air-cooled VRF unit (electric) with DX cooling coils and DX heating coils.

02: reversible air-cooled VRF unit (electric) with DX cooling coils and DX heating coils. The detailed results for IOhD, IOcD, CCOhR, CCOcR, cooling and heating energy use, and cooling and heating GHG emissions were given in the following sections.

3.1. How will indoor thermal comfort conditions vary due to climate change towards the end of the century?

The time-integrated thermal discomfort analysis of the reference building model provides insights into indoor environment parameters with different HVAC strategies for different weather scenarios. The indoor overheating and overcooling rates were calculated using IOhD and IOcD indicators. The IOhD and IOcD values for different HVAC strategies are shown in Fig. 9. The best case and worst case scenarios for IOhD and IOcD in reference building are represented in a background of light green and light red, respectively. The IOhD values for all three cooling strategies remain under 1.2 °C for different weather scenarios, whereas the IOcD values were as high as 3.9 °C for heating strategy 01 water boiler (electric) with heated floors.

Among the cooling strategies:

1. Baseline: air-cooled chiller (electric) with water cooling coils gave an IOhD value of 0.2 °C for 2010s_Current and 0.5 °C for 2090s_SSP5 with a 0.3 °C increase in overheating in the building.
2. Strategy 01: air-cooled chiller (electric) with chilled ceilings gave an IOhD value of 0.5 °C for 2010s_Current and 1.2 °C for 2090s_SSP5 with a 0.7 °C increase in overheating in the building.
3. Strategy 02: reversible VRF unit (electric) with DX cooling coils gave a value of 0.6 °C for 2010s_Current and 1.2 °C for 2090s_SSP5 with a 0.6 °C increase in overheating in the building.

In comparison with the baseline cooling strategy - air-cooled chiller (electric) with water cooling coils:

1. Strategy 01: air-cooled chiller (electric) with chilled ceilings gave a 0.3 °C increase for 2010s_Current and a 0.7 °C increase for 2090s_SSP5 in overheating in the building.
2. Strategy 02: reversible VRF unit (electric) with DX cooling coils gave a 0.4 °C increase for 2010s_Current and a 0.7 °C increase for 2090s_SSP5 in overheating in the building.

Among the heating strategies:

1. Baseline: water boiler (gas) with water heating coils gave an IOcD value of 1.2 °C for 2010s_Current and 0.5 °C for 2090s_SSP5 with a 0.7 °C decrease in overcooling in the building.

2. Strategy 01: water boiler (electric) with heated floors gave an IOcD value of 3.9 °C for 2010s_Current and 2.2 °C for 2090s_SSP5 with a 1.7 °C decrease in overcooling in the building.

3. Strategy 02: reversible VRF unit (electric) with DX heating coils gave an IOcD value of 0.4 °C for 2010s_Current and 0.3 °C for 2090s_SSP5 with a 0.1 °C decrease in overcooling in the building.

In comparison with the baseline heating strategy - water boiler (gas) with water heating coils:

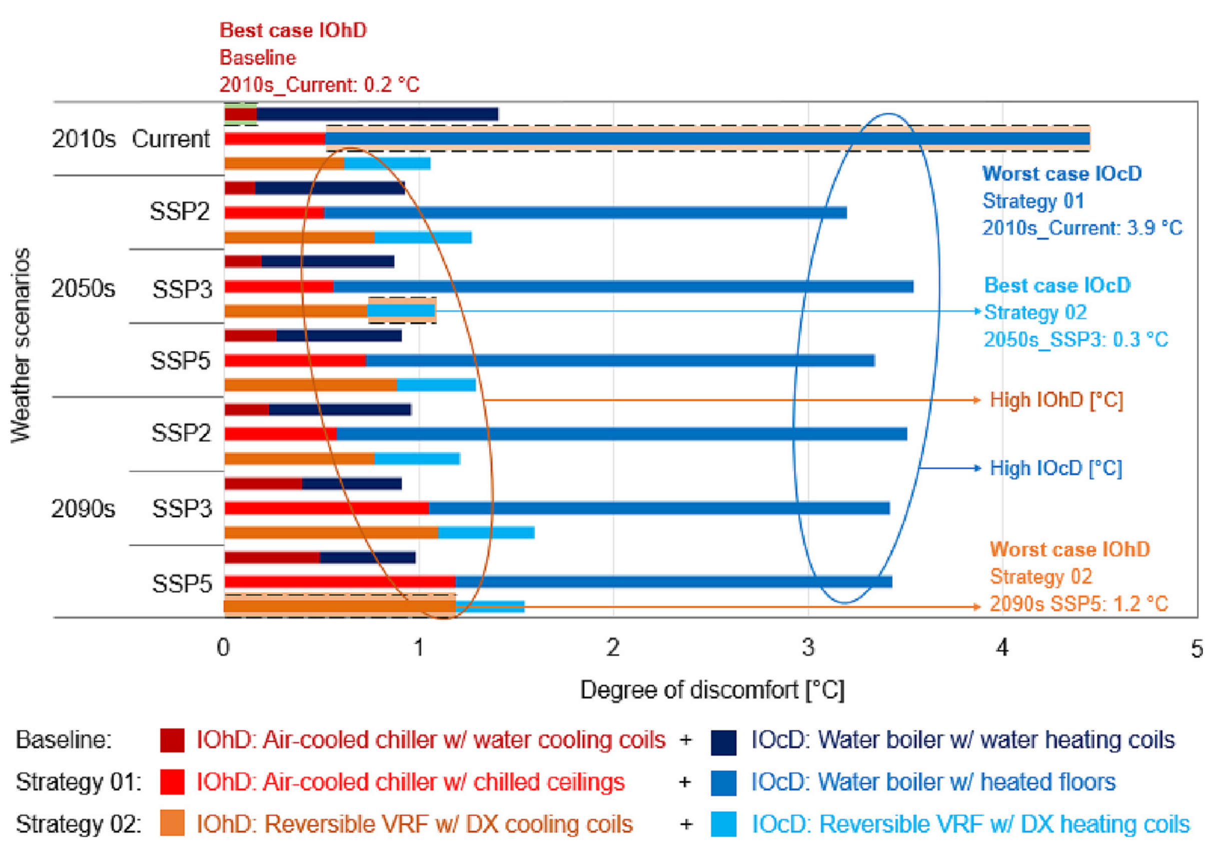

Fig. 9. IOhD [°C] and IOcD [°C] values for different HVAC strategies and various weather scenarios.

1. Strategy 01: water boiler (electric) with heated floors gave a 2.7 °C increase for 2010s_Current and a 1 °C increase for 2090s_SSP5 in overcooling in the building.
2. Strategy 02: reversible VRF unit (electric) with DX heating coils gave a 0.8 °C decrease for 2010s_Current and a 0.4 °C decrease for 2090s_SSP5 in overcooling in the building.

There is an increase in IOhD values from the 2010s_Current to the 2090_SSP5 scenario since the cooling effect of mechanical ventilation will decrease with an increase in outdoor temperature. The same effect however will contrarily impact the IOcD values and IOcD values decrease from 2010s_Current to 2090s_SSP5. The IOcD values in 2010s_Current are six times higher than IOhD for Baseline configuration. With climate change, this situation will be reversed for 2090s_SSP5 were IOhD and IOcD values become 0.5 °C, on par with each other. Hence, the reference building will become more and more uncomfortable during the summer than in winter with climate change. These findings are in line with findings from [35]. This increasing overheating discomfort could be met by decreasing the cooling setpoint from 26 °C to a lower value but this will also result in increased primary energy use and GHG emissions.

3.2. How will buildings resist overheating and overcooling due to climate change towards the end of the century?

The climate change resistivity was evaluated using CCOhR and CCOcR indicators using the weather scenarios 2010s_Current, 2050s_SSP5, and 2090s_SSP5. The results for each HVAC strategy are shown in Fig. 10. The best-case and worst-case scenarios for CCOhR and CCOcR in the reference building are represented in a background of light green and light red, respectively.

Among the cooling strategies:

1. Baseline: air-cooled chiller (electric) with water cooling coils gave a CCOhR value of 3.7.
2. Strategy 01: air-cooled chiller (electric) with chilled ceilings gave a CCOhR value of 1.8.
3. Strategy 02: reversible VRF unit (electric) with DX cooling coils gave a CCOhR value of 2.1.

Among the heating strategies:

1. Baseline: water boiler (gas) with water heating coils gave a CCOcR value of 2.6.

2. Strategy 01: water boiler (electric) with heated floors gave a CCOcR value of 1.1.

3. Strategy 02: reversible VRF unit (electric) with DX heating coils gave a CCOcR value of 20.2.

Since the CCOhR and CCOcR values for all three HVAC strategies were greater than one, the tested HVAC systems for the reference building were climate change resistant. This demonstrates that the cooling and heating strategies chosen and sized for the study will be capable of maintaining a suitable indoor thermal environment throughout the year, even during the worst-case scenarios towards the end of the century. Since the case study has active cooling strategies, it is more resistant to the effects of climate change, however with varying degrees of success. The Baseline with an air-cooled chiller with water cooling coils has the highest CCOhR with 3.7, making it the most resilient cooling strategy and demonstrating stronger resistance to climate change. Among the heating strategies, Strategy 03 reversible VRF unit with DX heating coils was the most resilient heating strategy with 20.2. Therefore, the study demonstrates that the choice of cooling and heating systems will have a significant impact on how comfortable a building will be in the future.

3.3. How will HVAC energy use and peak load demand shift due to climate change towards the end of the century?

The cooling and heating energy use of the reference building model was simulated in EnergyPlus. The primary energy use of different cooling and heating strategies for different weather scenarios is shown in Fig. 11. The best case and worst case scenarios for energy use in reference building are represented in a background of light green and light red, respectively.

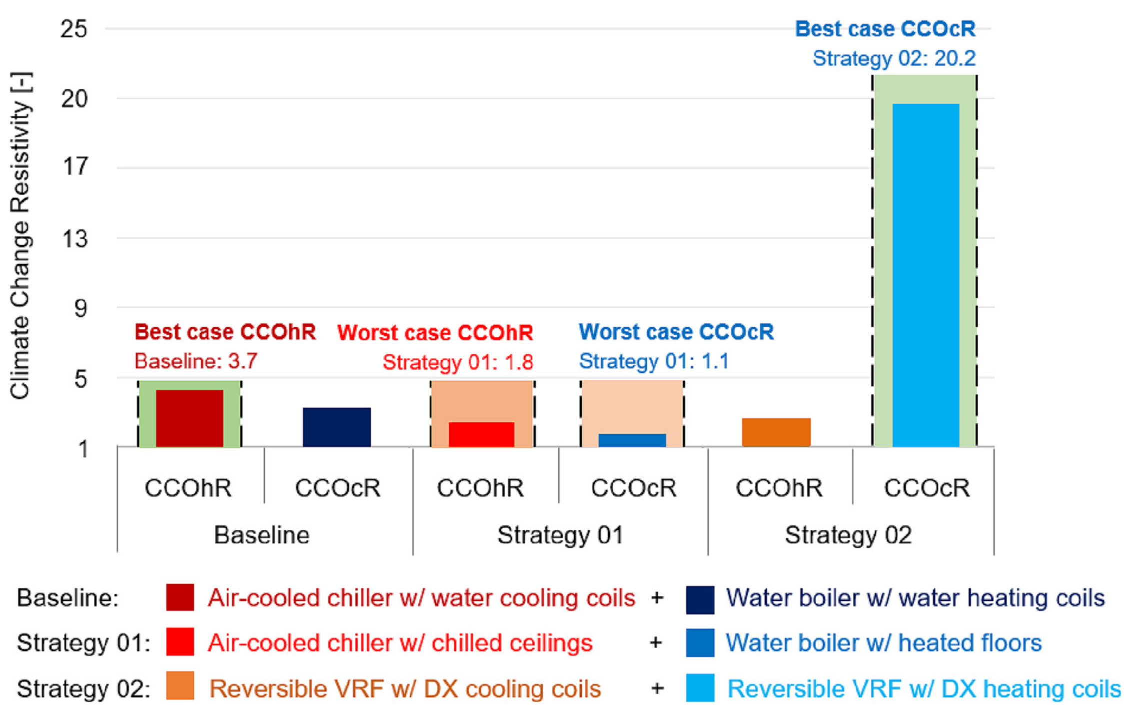

Fig. 10. Climate Change Overheating Resistivity (CCOhR) and Climate Change Overcooling Resistivity (CCOcR) values for different HVAC strategies using climate scenarios 2010s_Current, 2050s_SSP5, and 2090s_SSP5.

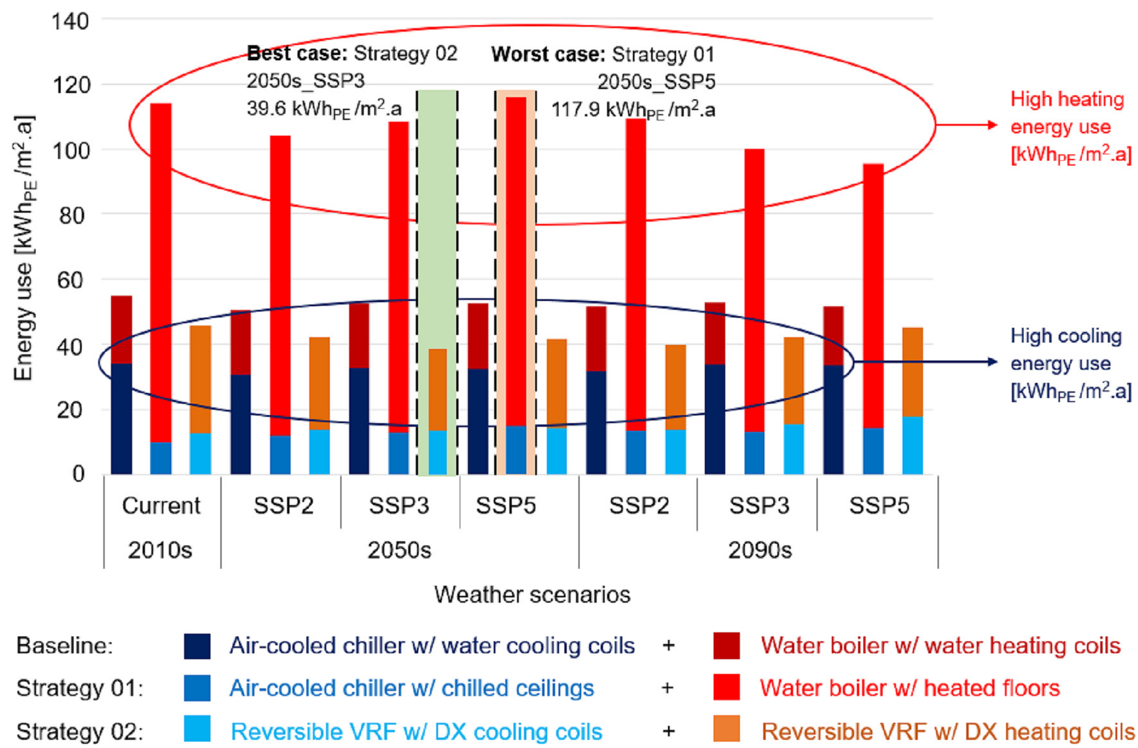

Fig. 11. Primary energy use [kWh$_{PE}$/m^2.a] for different HVAC strategies and various weather scenarios.

The primary cooling energy includes the energy used from the system fans in addition to the cooling system. Among the cooling strategies:

1. Baseline: air-cooled chiller (electric) with water cooling coils gave a primary cooling energy use of 34.1 kWh$_{PE}$/m^2.a for 2010s_Current and 33.7 kWh$_{PE}$/m^2.a for 2090s_SSP5 with a 0.4 kWh$_{PE}$/m^2.a decrease in primary cooling energy use in the building. The site cooling energy use for 2010s_Current and 2090s_SSP5 was 13.6 kWh/m^2.a and 13.5 kWh/m^2.a respectively.
2. Strategy 01: air-cooled chiller (electric) with chilled ceilings gave a primary cooling energy use of 10.1 kWh$_{PE}$/m^2.a for 2010s_Current and 14.3 kWh$_{PE}$/m^2.a for 2090s_SSP5 with a 4.2 kWh$_{PE}$/m^2.a increase in primary cooling energy use in the building. The site cooling energy use for 2010s_Current and 2090s SSP5 was 4 kWh/m^2.a and 5.7 kWh/m^2.a respectively.
3. Strategy 02: reversible VRF unit (electric) with DX cooling coils gave a primary cooling energy use of 12.8 kWh$_{PE}$/m^2.a for 2010s_Current and 17.9 kWh$_{PE}$/m^2.a for 2090s_SSP5 with a 5.1 kWh$_{PE}$/m^2.a increase in primary cooling energy use in the building. The site cooling energy use for 2010s_Current and 2090s_SSP5 was 5.1 kWh/m^2.a and 7.2 kWh/m^2.a respectively.

In comparison with the baseline cooling strategy - air-cooled chiller (electric) with water cooling coils:

1. Strategy 01: air-cooled chiller (electric) with chilled ceilings gave a 24 kWh$_{PE}$/m^2.a decrease for 2010s_Current and a 19.4 kWh$_{PE}$/m^2.a decrease for 2090s_SSP5 in primary cooling energy use in the building.
2. Strategy 02: reversible VRF unit (electric) with DX cooling coils gave a 21.3 kWh$_{PE}$/m^2.a decrease for 2010s_Current and a 15.8 kWh$_{PE}$/m^2.a decrease for 2090s_SSP5 in primary cooling energy use in the building.

Primary heating energy use includes the energy used from the system fans in addition to the heating system. Among the heating strategies:

1. Baseline: water boiler (gas) with water heating coils gave a primary heating energy use of 20.6 kWh$_{PE}$/m^2.a for 2010s_Current and 17.9 kWh$_{PE}$/m^2.a for 2090s_SSP5 with a 2.7 kWh$_{PE}$/m^2.a decrease in primary heating energy use in the building. The site heating energy use for 2010s_Current and 2090s_SSP5 was 14.6 kWh/m^2.a and 12 kWh/m^2.a respectively.

2. Strategy 01: water boiler (electric) with heated floors gave a primary heating energy use of 103.8 kWh$_{PE}$/m^2.a for 2010s_Current and 80.9 kWh$_{PE}$/m^2.a for 2090s_SSP5 with a 22.9 kWh$_{PE}$/m^2. a decrease in primary heating energy use in the building. The site heating energy use for 2010s_Current and 2090s_SSP5 was 41.5 kWh/m^2.a and 32.4 kWh/m^2.a respectively.

3. Strategy 02: reversible VRF unit (electric) with DX heating coils gave a primary heating energy use of 32.8 kWh$_{PE}$/m^2.a for 2010s_Current and 27.2 kWh$_{PE}$/m^2.a for the 2090s_SSP5 with a 5.6 kWh$_{PE}$/m^2.a decrease in primary heating energy use in the building. The site heating energy use for 2010s_Current and 2090s_SSP5 was 13.1 kWh/m^2.a and 10.9 kWh/m^2.a respectively.

In comparison with the baseline heating strategy - water boiler (gas) with water heating coils:

Strategy 01: water boiler (electric) with heated floors gave 83.2 kWh$_{PE}$/m^2.a increase for 2010s_Current and a 63 kWh$_{PE}$/m^2.an increase for 2090s_SSP5 in primary heating energy use in the building.
Strategy 02: reversible VRF unit (electric) with DX heating coils gave a 12.2 kWh$_{PE}$/m^2.an increase for 2010s_Current and a 9.3 kWh$_{PE}$/m^2.an increase for 2090s_SSP5 in primary heating energy use in the building.

Considering the energy performance in line with maintaining the indoor thermal environment, Strategy 02 with reversible VRF unit and DX cooling coils gave better performance for cooling. However, with climate change and increased outdoor temperatures, the energy performance of Strategy 02 started falling and has the highest energy use for the 2090s_SSP5 scenario. For heating, Strategy 02 with a reversible VRF unit with DX heating coils was again the preferred choice considering energy performance in line with maintaining the indoor thermal environment. The energy performance of Strategy 02 improves with climate change and increased outdoor temperatures and has the lowest energy use for the 2090s_SSP5 scenario. Even though climate-related parameters like CDD and HDD show more cooling hours than heating hours in the worst-case scenario of 2090s_SSP5, the building will remain as heating-dominated towards the end of the century.

The hourly peak primary cooling and heating demand [W_{PE}] for different HVAC strategies for different weather scenarios are shown in Fig. 12. The peak cooling demand was highest for Strategy 01: air-cooled chiller (electric) with chilled ceilings for 2090s_SSP5 with 149.3 W_{PE}. The peak heating demand was highest for Strategy 01: water boiler (electric) with heated floors for 2050s_SSP5 with 201 W_{PE}. The primary peak cooling and heating demand increased while using electricity as a source for heating compared to using natural gas as a source for heating. The best-case and worst-case scenarios for energy use in reference building are represented in a background of light green and light red, respectively. The hourly peak cooling/heating demand showed an increase of 244 W_{PE} between the best-case scenario and the worst-case scenario. In addition, the peak cooling demand will increase towards the end of the century, adding to summer peak cooling demand, and creating additional stress on electricity grids. Baseline heating uses natural gas as the source and Strategy 01 heating and Strategy 02 heating use electricity as the source. This transition considering the current electricity mix in Belgium will add to winter peak heating demand, creating additional stress on electricity grids.

3.4. How will buildings contribute to GHG emissions due to climate change towards the end of the century?

Following the building energy model simulation using EnergyPlus, GHG emissions from each HVAC strategy were calculated for different weather scenarios and in terms of annual CO_2 emissions in kg per square meter. The GHG emissions for different cooling and heating strategies for different weather scenarios are shown in Fig. 13. The best-case and worst-case scenarios for GHG emissions from the reference building are represented in a background of light green and light red, respectively.

The cooling GHG emissions include the emissions from the system fans in addition to the cooling system. Among the cooling strategies:

1. Baseline: air-cooled chiller (electric) with water cooling coils gave cooling GHG emissions of 9.2 kg.CO_2e/m^2.a for 2010s_Current and 9.1 kg.CO_2e/m^2.a for 2090s_SSP5 with a 0.1 kg.CO_2e/m^2.a decrease in cooling GHG emissions from the building.
2. Strategy 01: air-cooled chiller (electric) with chilled ceilings gave cooling GHG emissions of 2.7 kg.CO_2e/m^2.a for 2010s_Current and 3.9 kg.CO_2e/m^2.a for 2090s_SSP5 with a 1.2 kg.CO_2e/m^2.a increase in cooling GHG emissions from the building.
3. Strategy 02: reversible VRF unit (electric) with DX cooling coils gave cooling GHG emissions of 3.5 kg.CO_2e/m^2.a for 2010s_Current and 4.8 kg.CO_2e/m^2.a for 2090s_SSP5 with a 1.3 kg.CO_2e/m^2.a increase in cooling GHG emissions from the building.

In comparison with the baseline cooling strategy - air-cooled chiller (electric) with water cooling coils:

1. Strategy 01: air-cooled chiller (electric) with chilled ceilings gave a 6.5 kg.CO_2e/m^2.a decrease for 2010s_Current and a 5.2 kg.CO_2e/m^2.a decrease for 2090s_SSP5 in cooling GHG emissions from the building.

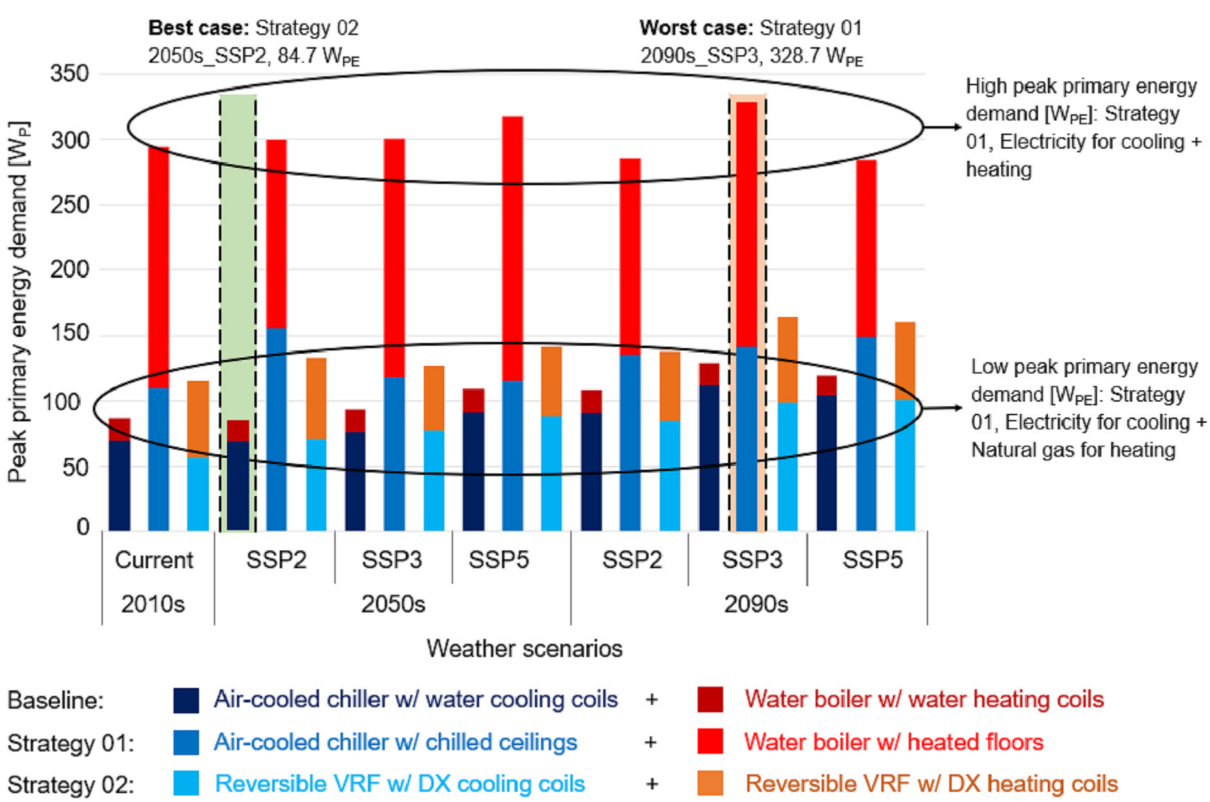

Fig. 12. Hourly primary peak load values [W_{PE}] for different cooling and heating strategies under various weather scenarios.

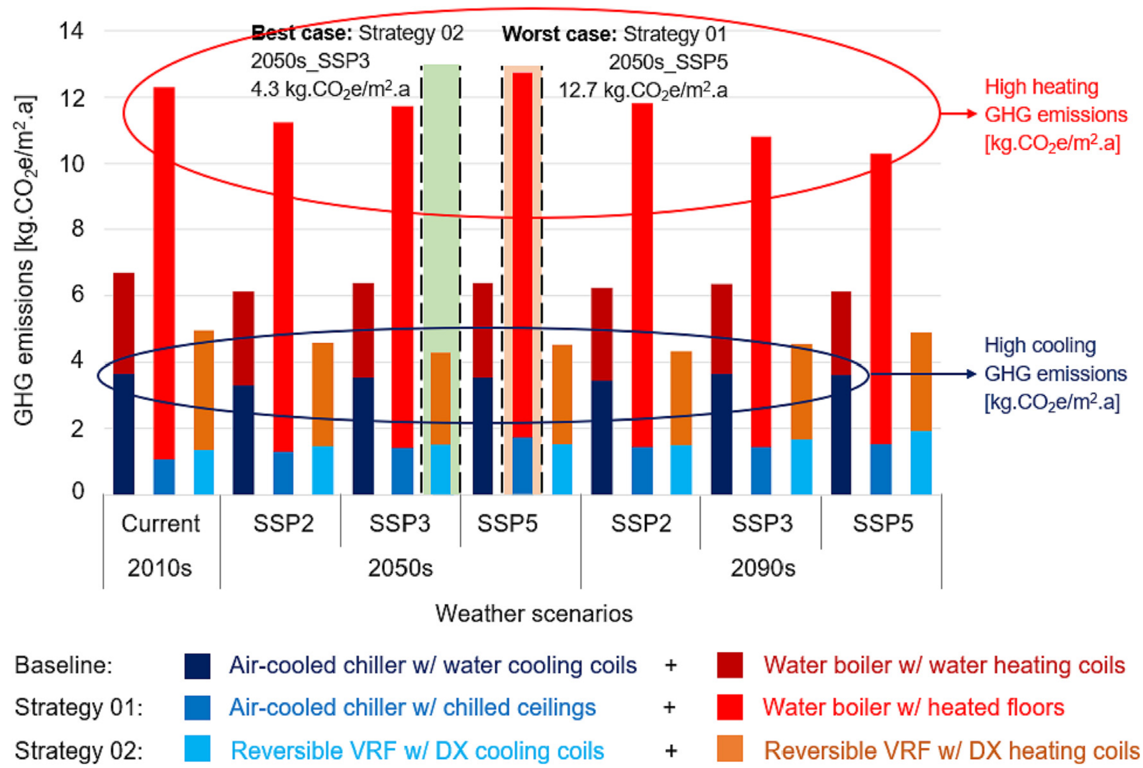

Fig. 13. GHG emissions [kg.CO_2e/m^2.a] from different HVAC strategies for various weather scenarios.

2. Strategy 02: reversible VRF unit (electric) with DX cooling coils gave a 5.7 kg.CO_2e/m^2.a decrease for 2010s_Current and a 4.3 kg.CO_2e/m^2.a decrease for 2090s_SSP5 in cooling GHG emissions from the building.

The heating GHG emissions include emissions from the system fans in addition to the heating system. Among the heating strategies:

1. Baseline: water boiler (gas) with water heating coils gave heating GHG emissions of 3 kg.CO_2e/m^2.a for 2010s_Current and 2.5 kg.CO_2e/m^2.a for 2090s_SSP5 with a 0.5 kg.CO_2e/m^2.a decrease in heating GHG emissions from the building.
2. Strategy 01: water boiler (electric) with heated floors gave heating GHG emissions of 11.2 kg.CO_2e/m^2.a for 2010s_Current and 8.7 kg.CO_2e/m^2.a for 2090s_SSP5 with 2.5 kg.CO_2e/m^2.a decrease in heating GHG emissions from the building.
3. Strategy 02: reversible VRF unit (electric) with DX heating coils gave heating GHG emissions of 3.5 kg.CO_2e/m^2.a for 2010s_Current and 2.9 kg.CO_2e/m^2.a for 2090_SSP5 with 0.6 kg.CO_2e/m^2.a decrease in heating GHG emissions from the building.

In comparison with the baseline heating strategy - water boiler (gas) with water heating coils:

1. Strategy 01: water boiler (electric) with heated floors gave 8.2 kg.CO_2e/m^2.a increase for 2010s_Current and a 6.2 kg. CO_2e/m^2.a increase for 2090s_SSP5 in heating GHG emissions from the building.
2. Strategy 02: reversible VRF unit (electric) with DX heating coils gave 0.5 kg.CO_2e/m^2.a increase for 2010s_Current and a 0.4 kg. CO_2e/m^2.a increase for 2090s_SSP5 in heating GHG emissions from the building.

4. Discussions

This section presents the primary findings, recommendations, strengths and limitations, and implications for practice and future work based on the study findings.

4.1. Main findings

1. Time-integrated thermal discomfort analysis indicated a substantial increase in overheating discomfort and a substantial decrease in overcooling discomfort by the end of the century. This means that climate change negatively impacts summer comfort and positively impacts winter comfort in mixed humid climates. This deteriorating summer comfort in buildings in mixed humid climates (4A) will be worsened in the future due to the increase in occupancy density, aging population, growing comfort expectations, and the urban heat island effect [88–90].
2. Indoor overheating assessment has shown that air-cooled chiller (electric) with water cooling coils gave the best performance among cooling systems with 0.49 °C for the worst-case scenario towards the end of the century (2090s_SSP5), whereas indoor overcooling assessment has shown that reversible VRF unit (electric) with DX heating coils gave the best performance among heating systems with 0.35 °C during the current scenario (2010s_Current).
3. Climate change resistivity assessment with different HVAC strategies proved that the building was resistant to overheating and overcooling due to future climate change. Among the three cooling strategies, the Baseline: air-cooled chiller (electric) with water cooling coils was found to be the most resistant to climate change induced overheating with a value of 3.7. Among the three heating strategies,

Strategy 02: reversible VRF unit (electric) with DX heating coils was found to be most resistant to climate change induced overcooling with a value of 20.2.
4. Evaluating the primary energy performance of cooling strategies, Strategy 01: air-cooled chiller (electric) with chilled ceilings gave a better primary cooling energy use of 14.3 kWh_{PE}/m^2.a for the worst-case scenario towards the end of the century (2090s_SSP5). However, the implementation of the cooling system from Strategy 01 in the reference building will require major renovation including the building structure including the floors. Hence, the study recommends Strategy 02: reversible VRF unit (electric) with DX cooling coils with primary cooling energy use of 17.9 kWh_{PE}/m^2.a for the same scenario.
5. Evaluating the primary energy performance of heating strategies, Baseline: water boiler (gas) with water heating coils gave a better performance with the primary heating energy use of 20.6 kWh_{PE}/m^2.a for the current scenario (2010s_Current). However, based on upcoming natural gas legislations from the European Commission that aim to shift away from fossil gas and more toward sustainable energy sources [84], we recommend Strategy 02: reversible VRF unit (electric) with DX heating coils with primary heating energy use of 32.8 kWh_{PE}/m^2.a for the same scenario.
6. The evaluation of primary peak cooling and heating demand showed a considerable increase while using electricity as a source for heating compared to using natural gas as a source for heating. The hourly peak cooling demand [W_{PE}] showed a 244 W_{PE} increase between the best-case scenario and the worst-case scenario among the tested HVAC strategies. This indicated that there will be growing stress on existing electricity grids to meet the peak cooling and heating demand.
7. Considering the GHG emissions among the cooling strategies, Strategy 01: air-cooled chiller (electric) with chilled ceilings gave a better emission rate of 3.9 $kg.CO_2e/m^2$.a for the worst-case scenario towards the end of the century (2090s_SSP5). However, for the same reasons stated in the case of primary cooling energy use, the study recommends Strategy 02: reversible VRF unit (electric) with DX cooling coils with an emission rate of 4.8 $kg.CO_2e/m^2$.a for the same scenario.
8. Heating GHG emissions were also in line with the primary heating energy use and among the heating strategies, Baseline: water boiler (gas) with water heating coils gave a better emission rate of 3 $kg.CO_2e/m^2$.a for the current scenario (2010s_Current). However, for the same reasons stated in the case of primary heating energy use, the study recommends Strategy 02: reversible VRF unit (electric) with DX heating coils with an emission rate of 3.5 $kg.CO_2e/m^2$.a for the same scenario.
9. The primary energy use and GHG emissions from these systems can be drastically reduced through the integration of renewable energy sources and other low-carbon emission sources like nuclear energy [90]. The biggest roadblock to electricity-based heating and the biggest reason for dependence on natural gas is the high primary energy value related to electricity use. The future emission factor for electricity will reduce with an increase in the integration of renewable energy [91,92].
10. The projected weather scenarios for Brussels indicated an increase in the mean annual air temperature of 1.33 °C by 2050s and 2.46 °C by 2090s. As climate change continues, summer will be stretched deeper into the other seasons with an increase in overheating [35,93], whereas winter will become warmer, with higher outdoor air temperatures being a much more common phenomenon in mixed humid climates (4A) in Europe.

4.2. Recommendations

1. The Baseline HVAC strategy with an air-cooled chiller (electric) with water cooling coils is constantly performing very well against the degree of discomfort. However, it is not recommended in practice anymore. Future applications should separate the ventilation from thermal conditioning to address variance and flexibility, meeting maximum hygienic airflow demand, which was not optimal compared to the air renewal rate. Future designs must modify the configuration and separate hygienic ventilation and thermal treatment.
2. Based on the observations from the study, reversible VRF systems with DX cooling coils and DX heating coils are recommended for future building constructions and renovations. This recommendation is based on time-integrated overheating and overcooling performance, climate change resistivity, energy use, and GHG emissions. Furthermore, the ventilation system in this strategy is separated from indoor thermal load maintenance and is focused solely on hygienic air quality.
3. Since the heated floors and chilled ceilings are two different kinds of radiant systems, it is recommended to not use them together as in the implementation of Strategy 01. Either floor heating should be installed, which can also be used for cooling, or radiant ceiling panels should be used, which may be used for heating purposes. SAPPceiling with integrated radiant cooling and heating panels is suggested as an appropriate technology for future studies and applications considering the environmental impact [94,95].
4. Replacing the water boiler with an air-to-water heat pump can be the solution to improve the performance of the Strategy 01 heating configuration that uses heated floors. Since the water temperature for the heated floor was around 28.5 °C, according to the model, the boiler should work in part load, since the boilers are usually designed to provide hot water at 30 to 55 °C water, which in this case was not efficient. Furthermore, the overnight schedule of heated floors adopted to avoid time lag of heat movement in the building added to the inefficient performance of the heated floors. For future applications, the heated floor operation schedule should coincide with occupancy and daytime for commercial buildings so that it will be appended by internal equipment, occupant, and solar gains. For building heating, electric heaters are also a much more efficient system compared to electric boilers.
5. The modulated continuous schedule of 23*h*00 to 07*h*00 for Strategy 01 would be effective for cooling purposes, since the cooling occurs when heat gains are absent and the outside temperature is lower, preparing the building to absorb heat gains in the morning. However, it is not recommended for heating purposes, since the building was heated during no occupancy and it is advised to heat more during the day in the presence of heat gains, which will reduce the heating demand.
6. The real-time monitoring and measurement of peak loads in the buildings is a significant process. This monitoring will require a minute by minute submetering system. The current state of the art of the cooling and heating energy use submetering employs an ultrasonic measuring and microprocessor technology. A single board submetering will comprise calculations for flow measuring circuits. Unfortunately, this advanced technology is not available in most newly constructed buildings. Future construc-

tions and renovations should implement these technologies, as peak load is an important parameter that can be used to calibrate building models with real building performance.

4.3. Strengths and limitations

The main strength of the paper was that the paper proposed and implemented a climate change sensitive approach used to select and size the HVAC systems, coupled with the choice of optimal sizing factor. The eventual performance evaluation of different HVAC systems showed that these systems were resistant to climate change considering the worst-case scenarios towards the end of the century. This resistivity of HVAC systems was credited to the above-mentioned approach.

The study used a calibrated reference building model using monthly energy use values according to ASHRAE Guideline 14 [78]. This increased the reliability of model outputs in comparison to real-world outputs in terms of building performance. The study compared three commonly used HVAC strategies in terms of building performance parameters and identified the best strategy, whereas the existing literature that addressed climate change effects on building performance was formulated based on the unique assumption of HVAC systems. Based on the findings of the paper, future research can focus on developing nZEBs that are energy-efficient, carbon–neutral, and provide occupant thermal comfort for changing climate scenarios.

Any study that evaluates the impacts of climate change must use accurate data on the past, present, and future climate, as this determines the quality of the study [58]. The climate data was one of the strengths of this study, as it was based on the Modele Atmospherique Regional, MAR from the University of Liege, which has a high spatial resolution of around 5 km and was specifically developed for Belgium. The study was based on a real nZEB used as an office located near Brussels, Belgium, and represents the mixed humid climate (4A) according to the ASHRAE 169 classification [46]. This classification adds to the reliability of the study as this method using CDD and HDD was more adapted to predict energy use in the buildings.

Some of the limitations were that the study only considered periods like the 2010s, 2050s, and 2090s based on SSPs like SSP2, SSP3, and SSP5, and did not consider intermediate periods like 2030s, and 2070s, etc., along with other SSP scenarios like SSP1 and SSP4. This case study was conducted on a single reference building located in Brussels, Belgium. Whilst this study was only focused on Brussels in Belgium, similarities can be drawn to other locations with similar climate conditions. Hence, this paper provides valuable insights and opens the door for future studies. Furthermore, due to unavailability of peak load data from the real building, the reference building model was calibrated for monthly electricity and natural gas use even though peak loads are considered as a KPI in the study. Peak load measurement and monitoring is significant and requires submetering, which was not available in the nearly zero-energy office building used in this study.

4.4. Implications for practice and work

1. More HVAC strategies and configurations including production and distribution sides should be assessed to create a comprehensive database on which strategy was more suited depending on the building type, category, location, etc.
2. The findings from the study strongly suggest a substantial increase in overheating discomfort and a substantial decrease in overcooling discomfort by the end of the century in mixed humid climates. This indicates that passive cooling systems alone will not be capable of resisting building overheating due to climate change.
3. The studies also indicate that the building HVAC systems should be sized taking into consideration the effects of climate change. This in turn will help the buildings to be resistant to the long-term effects of climate change.
4. HVAC design and sizing in the future should be based on climate files that consider events like heatwaves and urban heat island effects. This will ensure thermal comfort and energy efficiency in the buildings during extreme events.
5. Electric heating will use more primary energy than natural gas heating in Belgium. However, future patterns of using electricity for heating should assume that electricity will largely come from renewable energy sources like solar, wind, etc. [92].
6. Future studies should focus more on simulation and field studies in office buildings located in mixed humid climates (4A) to create a better understanding of the impacts of long-term climate change and short-term weather events like heatwaves on building performance.
7. Existing indices like IOhD and IOcD must be developed to include parameters like relative humidity and air velocity, along with personal parameters like metabolic rates and clothing factors. Thermal comfort was highly dependent on human perception, and the introduction of personalized factors into existing indices will improve the quality of thermal comfort assessments [96].
8. Since the weather data was an important parameter that will determine the quality of the study, it is important to analyze how the future climate files from different sources like the MAR, Meteonorm, CORDEX, CCWorldWeatherGen, and WeatherShift vary with each other.
9. The results from the study can be used for future revisions of the building codes and regulations with provisions regarding active cooling system use. These revisions should include time-integrated overheating criteria and the necessity of active cooling systems installation coupled with renewable energy sources in line with EU regulations and roadmaps [97].
10. European Environment Agency (EEA) forecasts that by 2030, the share of renewable electricity in total power generation could reach 70%, enabling a net reduction in GHG emissions of 55% and achieving climate neutrality by 2050 [98]. The paper recommends a shift in energy use to attain these goals.
11. The findings from this study can be used for the early-stage design of nearly zero-energy office buildings in other European cities like London, Madrid, Milan, and Paris, among others, that share a mixed humid climate, similar to the study location.

5. Conclusions

This study carried out a climate change impact evaluation in terms of time-integrated discomfort, climate change resistivity, energy efficiency, and GHG emissions on a nearly zero-energy office building in Brussels, Belgium. The building performance was analyzed for three different HVAC strategies using seven weather scenarios including 2010s_Current, 2050s_SSP2, 2050s_SSP3, and 2050s_SSP5, and 2090s_SSP2, 2090s_SSP3, and 2090s_SSP5, based on the regional climatic model MAR. The results show that there will be a significant increase in building overheating and cooling energy use, and a substantial decrease in building overcooling and heating energy use in the future in the reference building used in this study. Implementation of resilient cooling systems [99] in buildings should be focused on in this scenario. Notably, all three HVAC strategies assessed in the study proved to be resistant to climate change induced overheating and overcooling due to climate change sensitive sizing and design.

By the 2090s, the overheating risk, as measured by the Indoor Overheating Degree (IOhD) metric, will rise to a maximum of 1.2 °C, while the overcooling risk will fall to a minimum of 0.3 °C. Under the high emission scenario or 2090s_SSP5, it is predicted that the overheating risk will be more prevalent than the overcooling risk. Furthermore, It is predicted that under the high emission scenario, i.e., 2090s SSP5, the primary cooling energy usage with electricity for HVAC systems would rise to 13.5 kWh/m^2, while the primary heating energy use with natural gas will fall to 10.9 kWh/m^2. Additionally, the cooling GHG emissions are predicted to be 3.9 kg.CO_2e/m^2.a and the heating GHG emissions to be 3.5 kg.CO_2e/m^2.a. Therefore, the study predicts higher indoor overheating risks with increased primary cooling energy consumption, and lower indoor overcooling risks with primary heating energy use towards the end of the century.

With upcoming natural gas legislation packages from the European Commission aiming to steer away from fossil gas and towards more sustainable energy sources [86], the paper foresees a transition of HVAC fuel from natural gas to electricity, especially for heating purposes. The future emission factor for electricity will reduce with the increase in the integration of renewable energy in the Belgian energy mix [92]. To accelerate and contribute toward the EU objective of reducing emissions by 55% by the 2030s [98], the paper suggests increased integration of renewables and renovation of traditional building systems. This will help to decrease the stress on existing electricity grids to meet the increasing energy demand in the future. Future studies should conduct a deeper analysis of how climate change responsive HVAC sizing based on design days affects the thermal environment and energy performance in buildings with different HVAC strategies in different climate zones.

Data availability

Data will be made available on request.

Declaration of Competing Interest

The authors declare the following financial interests/personal relationships which may be considered as potential competing interests:

Deepak Amaripadath reports financial support was provided by Walloon Public Service. Deepak Amaripadath reports financial support was provided by MK Engineering.

The remaining authors declare that they have no known competing financial interests or personal relationships that could have appeared to influence the work reported in this paper.

Acknowledgments

The European researchers were funded by the Service Public de Wallonie (SPW), Belgium, under BElgian WAllonia REsearch (BEWARE) fellowships and European Union (EU) framework program for research and innovation, Marie Skłodowska-Curie Actions (MSCA) through contract no. 847587. The authors would like to gratefully acknowledge the Walloon Region, EU MSCA, and MK Engineering for the Project SurChauffe funding. We would like to thank the stakeholders of Project OCCuPANt. We also acknowledge Clinic Saint-Pierre, for their support for the case study. We would like to acknowledge the Sustainable Building Design Lab at the Faculty of Applied Sciences at the University of Liege for the valuable support and use of the state-of-the-art SCORPION for building performance simulations and data analysis. This study was a part of the IEA Energy in Buildings and Communities (EBC) Annex 80 - Resilient Cooling of Buildings.

Appendix A

Table A.1 lists the design weather data with respect to ISO 15927-2 [36] for different TMYs according to different SSP scenarios for HVAC sizing. The wet bulb temperature is calculated using [100,101].

Appendix B

Table B.1 summarizes the characteristics of the reference building used for the current study. The characteristics and assumptions of different HVAC strategies that were evaluated in the study are listed in Table B.2. The VRF unit has a COP of 3.3 for cooling and 3.4 for heating. These values were obtained from the existing energy efficiency standards [102]. The water boiler used in this study uses a COP of 0.9. This value was obtained from a factsheet released by the Department of Climate Change, Energy, the Environment and Water, Australia [103].

Table A1
Design day weather data with respect to ISO 15927-2 [36] for TMYs according to different SSP scenarios.

TMYs	Winter design weather data	Summer design weather data
2010s_Current	Maximum Dry bulb temperature: −10 °C Wind speed: 3.4 m/s Wind direction: 55.7 °N	Maximum Dry bulb temperature: 36.9 °C Wet bulb temperature: 23.3 °C Minimum Dry bulb temperature: 20.6 °C
2050s_SSP2	Maximum Dry bulb temperature: −6.4 °C Wind speed: 0.5 m/s Wind direction: 88.4 °N	Maximum Dry bulb temperature: 39.6 °C Wet bulb temperature: 21.9 °C Minimum Dry bulb temperature: 27.6 °C
2050s_SSP3	Maximum Dry bulb temperature: −11.4 °C Wind speed: 1.9 m/s Wind direction: 105.4 °N	Maximum Dry bulb temperature: 39.5 °C Wet bulb temperature: 22.9 °C Minimum Dry bulb temperature: 19.9 °C
2050s_SSP5	Maximum Dry bulb temperature: −8.7 °C Wind speed: 6.5 m/s Wind direction: 54.2 °N	Maximum Dry bulb temperature: 35.8 °C Wet bulb temperature: 22.4 °C Minimum Dry bulb temperature: 23.4 °C
2090s_SSP2	Maximum Dry bulb temperature: −12.7 °C Wind speed: 2.4 m/s Wind direction: 37.4 °N	Maximum Dry bulb temperature: 35 °C Wet bulb temperature: 22.2 °C Minimum Dry bulb temperature: 20.6 °C
2090s_SSP3	Maximum Dry bulb temperature: −8.8 °C Wind speed: 1.5 m/s Wind direction: 18.5 °N	Maximum Dry bulb temperature: 42.9 °C Wet bulb temperature: 22.6 °C Minimum Dry bulb temperature: 19.6 °C
2090s_SSP5	Maximum Dry bulb temperature: −2.1 °C Wind speed: 2.6 m/s Wind direction: 135 °N	Maximum Dry bulb temperature: 41.9 °C Wet bulb temperature: 21.8 °C Minimum Dry bulb temperature: 26.5 °C

Table B1
General description of reference nearly zero-energy building used in the case study.

Description	Value
Number of floors	4, including an underground parking area
Total area [m^2]	4507
Conditioned area [m^2]	2803
Unconditioned area [m^2]	1704
Interior volume [m^3]	10,115
Exterior volume [m^3]	12,169
Window-wall ratio [%]	38.25
Window U-value [W/m^2K]	0.50
Window G-value [-]	0.50
Solar Heat Gain Coefficient (SHGC) [-]	0.66
External wall U-value [W/m^2K]	0.35
Roof U-value [W/m^2K]	0.25
Ground floor U-value [W/m^2K]	0.25
Basement floor U-value [W/m^2K]	0.78
Airtightness (50 Pa.m^3/h.m^2) [ACH]	0.60

Appendix C

The quality of the reference nearly zero-energy building model used in this study was ensured through calibration as per the ASHRAE 14 Guideline using real monthly energy use data for natural gas and electricity use collected in 2019 [72]. The ASHRAE Guideline 14 assesses the goodness-of-fit of the building energy model using two indices [78]. These indices are the Normalized Mean Bias Error (NMBE) and the Root Mean Square Error Coefficient (CV (RMSE)). NMBE is a percentage value that indicates the overall bias error between measured and simulated data for a known time resolution. CV(RMSE) is a percentage that represents how well the simulation model describes the variability in the measured data. Monthly electricity use had NMBE and CV(RMSE) values of 2.1% and 14.2%, and monthly natural gas use had 2.1% and 12.8%, which were both within the acceptable ranges of 5% and 15% mandated by ASHRAE Guideline 14 [78]. The calibration process went through several rounds of coauthor reviews to further ensure the quality of the reference model used in the study. Table C.1 lists the calibration values for the building reference model with NMBE [%] and CV(RMSE) [%] according to ASHRAE Guideline 14 [78]. The calibration results for the reference nearly zero-energy building for site electricity use [kWh] and site natural gas use [kWh] for the year 2019 are shown in Fig. C.1.

Appendix D

As per the cooling capacity curve for the study configuration, when outdoor temperature increases the cooling capacity increases, and as per the heating capacity curve, when outdoor temperature decreases, the heating capacity increase [104]. The capacity ratio modifier of temperature curves for cooling and heating is shown in Fig. D.1. The minimum and maximum outdoor temperatures in the cooling mode were −6 °C and 43 °C. The minimum and maximum outdoor temperatures in the heating mode were −20 °C and 40 °C.

Table B2
The DesignBuilder model inputs for HVAC strategies: (i) Baseline: air-cooled chiller (electric) with water cooling coils and a water boiler (gas) with water heating coils, (ii) Strategy 01: air-cooled chiller (electric) with chilled ceilings and a water boiler (electric) with heated floors, and (iii) Strategy 02: reversible VRF unit (electric) with DX cooling coils and DX heating coils.

Parameters	Baseline	Strategy 01	Strategy 02
Cooling			
Target zones	Office rooms, meeting rooms, cafeterias, and multipurpose hall		
Cooling [°C]	Setpoint: 26 °C [51], Setback: 50 °C		
Production	Air-cooled chiller	Air-cooled chiller	Reversible VRF unit
Nominal COP	5.5	5.5	3.3 [102]
Distribution	Water cooling coils	Chilled ceilings	DX cooling coils
Fuel type	Electricity	Electricity	Electricity
Sizing factor	1	1	1
Schedule	On: Weekdays, 07*h*00−17*h*00 Off: Weekends & Oct.-Apr.	On: Weekdays, 23*h*00−07*h*00 Sundays, 23*h*00−24*h*00 [83] Off: Weekends & Oct. - Apr.	On: Weekdays, 07*h*00−17*h*00 Off: Weekends & Oct. - Apr.
Heating			
Target zones	Office rooms, meeting rooms, forum, cafeterias, and multipurpose hall		
Heating [°C]	Setpoint: 23 °C, Setback: 19 °C		
Production	Water boiler	Water boiler	Reversible VRF unit
Nominal COP	0.9 [103]	0.9 [103]	3.4 [102]
Distribution	water heating coils	Heated floors	DX heating coils
Fuel type	Natural gas	Electricity	Electricity
Sizing factor	1	1	1
Schedule	On: Weekdays, 07*h*00 −17*h*00 Off: Weekends & May-Sep.	On: Weekdays, 23*h*00−07*h*00 Sundays, 23*h*00−24*h*00 [83] Off: Weekends & May-Sep.	On: Weekdays, 07*h*00−17*h*00 Off: Weekends & May-Sep.
Ventilation: AHU1 - offices and other spaces, AHU2 - multipurpose hall			
Target zones	Zone 1: Office rooms, meeting rooms, forum, cafeterias, and multipurpose hall Zone 2: Halls, stairways, circulations, and lavatories		
Ventilation rates (m^3/hr)	21,600	9000 [51]	9000 [51]
AHU type	Variable Air Volume (VAV) unit		
AHU fans	Variable volume fans		
Nominal COP	0.7	0.7	0.7
Schedule	On: Weekdays, 07*h*00−17*h*00 Off: Weekends	On: Weekdays, 07*h*00−17*h*00 Off: Weekends	On: Weekdays, 07*h*00−17*h*00 Off: Weekends

Table C1
NMBE [%] and CV(RMSE) [%] for the building simulation model after calibration for the year 2019.

Year	Electricity		Natural gas	
	NMBE [%]	CV(RMSE) [%]	NMBE [%]	CV(RMSE) [%]
2019	2.1	14.2	2.1	12.8

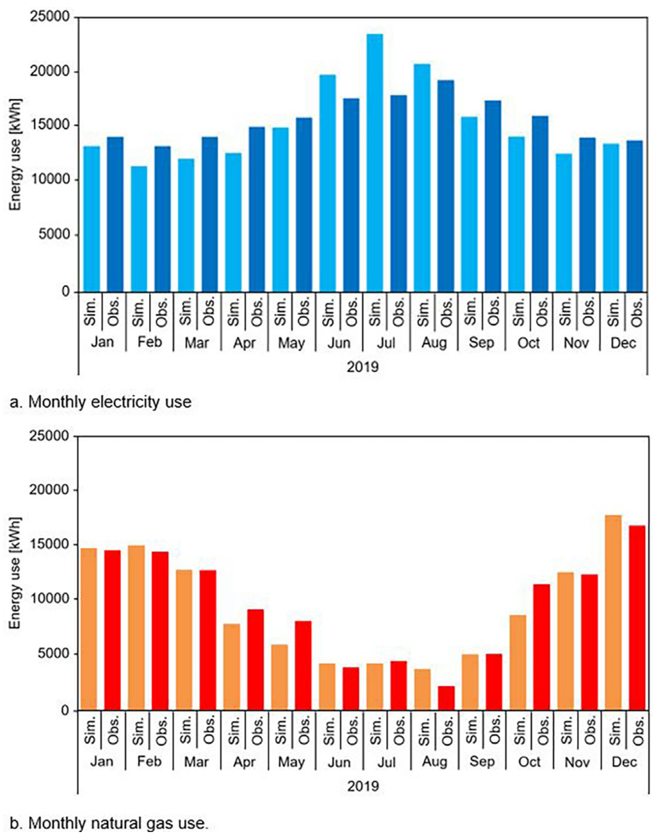

Fig. C1. Reference nearly zero-energy building calibration results for electricity and natural gas use for the year 2019.

References

[1] M. Santamouris, Innovating to zero the building sector in Europe: minimising the energy consumption, eradication of the energy poverty and mitigating the local climate change, Sol. Energy 128 (2016) 61–94, https://doi.org/10.1016/j.solener.2016.01.021.

[2] D. D'Agostino, D. Parker, I. Epifani, D. Crawley, L. Lawrie, How will future climate impact the design and performance of nearly Zero Energy Buildings (nZEBs)?, Energy 240 (2022), https://doiorg/10.1016/j.energy.2021.122479.

[3] A. Robert, M. Kummert, Designing net-zero energy buildings for the future climate, not for the past, Build. Environ. 55 (2012) 150–158, https://doi.org/10.1016/j.buildenv.2011.12.014.

[4] H.M. Füssel, Adaptation planning for climate change: concepts, assessment approaches, and key lessons, Sustain. Sci. 2 (2) (2007) 265–275, https://doi.org/10.1007/s11625-007-0032-y.

[5] OE&H, "Anthropogenic climate change," NSW Office of Environment & Heritage, 2017. [online]. Available: www.environment.nsw.gov.au/threatenedspeciesapp/profile.aspx?id=20025, Accessed on: Mar. 15, 2022.

[6] J. Mccarthy, O. Canziani, N. Leary, D. Dokken, K. White, "Climate change 2001: Impacts, adaptation, and vulnerability," Contribution of Working Group II to the Fourth Assessment Report of the Intergovernmental Panel on Climate Change, vol. 19, Jul. 2001.

[7] S.I. Bohnenstengel, S. Evans, P.A. Clark, S.E. Belcher, Simulations of the London urban heat island, Q. J. R. Meteorolog. Soc. 137 (659) (2011) 1625–1640, https://doi.org/10.1002/qj.855.

[8] T.R. Oke, "The heat island of the urban boundary layer: characteristics, causes and effects," *in Wind Climate in Cities*, J. E. Cermak, A. G. Davenport, E. J. Plate, and D. X. Viegas, eds. Dordrecht: Springer Netherlands, 1995, pp. 81–107, doi: 10.1007/978-94-017-3686-2_5.

[9] M. Santamouris et al., Urban heat island and overheating characteristics in Sydney, Australia. An analysis of multiyear measurements, Sustainability 9 (5) (2017), https://doi.org/10.3390/su9050712.

[10] L.F. Cabeza, D. Ürge-Vorsatz, The role of buildings in the energy transition in the context of the climate change challenge, Global Transitions 2 (2020) 257–260, https://doi.org/10.1016/j.glt.2020.11.004.

[11] C. Huynh, "How green buildings can help fight climate change," USGBC, 2021. [online]. Available: www.usgbc.org/articles/how-green-buildings-can-help-fight-climate-change, Accessed on: Mar. 21, 2022.

[12] K. Bamdad, M.E. Cholette, S. Omrani, J. Bell, Future energy-optimised buildings - Addressing the impact of climate change on buildings, Energ. Build. 231 (2021), https://doi.org/10.1016/j.enbuild.2020.110610.

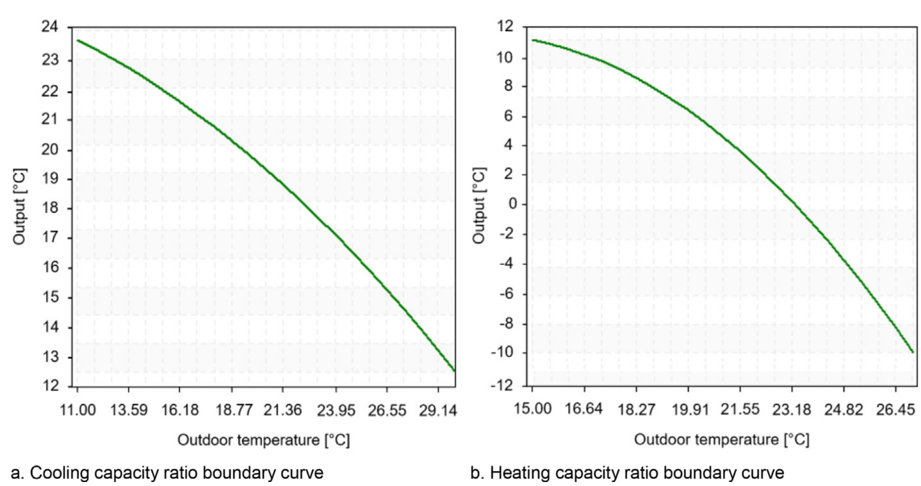

Fig. D1. VRF system capacity ratio modifier function of temperature curves.

[13] A. Jiang, X. Liu, E. Czarnecki, C. Zhang, Hourly weather data projection due to climate change for impact assessment on building and infrastructure, Sustain. Cities Soc. 50 (2019), https://doi.org/10.1016/j.scs.2019.101688.
[14] D. Daly, P. Cooper, Z. Ma, Implications of global warming for commercial building retrofitting in Australian cities, Build. Environ. 74 (2014) 86–95, https://doi.org/10.1016/j.buildenv.2014.01.008.
[15] I. Andrić, M. Koc, S.G. Al-Ghamdi, A review of climate change implications for built environment: impacts, mitigation measures and associated challenges in developed and developing countries, J. Clean. Prod. 211 (2019) 83–102, https://doi.org/10.1016/j.jclepro.2018.11.128.
[16] L. Guan, Implication of global warming on air-conditioned office buildings in Australia, Build. Res. Inf. 37 (1) (2009) 43–54, https://doi.org/10.1080/09613210802611025.
[17] L. Guan, The implication of global warming on the energy performance and indoor thermal environment of air-conditioned office buildings in Australia, Queensland University of Technology, Brisbane, Australia, 2006, Ph.D. Thesis, [Online]. Available:.
[18] M. Ferreira, M. Almeida, A. Rodrigues, S.M. Silva, Comparing cost-optimal and net-zero energy targets in building retrofit, Build. Res. Inf. 44 (2) (2016) 188–201, https://doi.org/10.1080/09613218.2014.975412.
[19] M. Ferreira, M. Almeida, Benefits from energy related building renovation beyond costs, energy and emissions, Energy Procedia 78 (2015) 2397–2402, https://doi.org/10.1016/j.egypro.2015.11.199.
[20] J. Chai, P. Huang, Y. Sun, Differential evolution - based system design optimization for net zero energy buildings under climate change, Sustain. Cities Soc. 55 (2020), https://doi.org/10.1016/j.scs.2020.102037.
[21] S. Longo, F. Montana, E. Riva Sanseverino, A review on optimization and cost-optimal methodologies in low-energy buildings design and environmental considerations, Sustain. Cities Soc. 45 (2019) 87–104, https://doi.org/10.1016/j.scs.2018.11.027.
[22] W. O'Brien, A. Athienitis, Modeling, Design, and Optimization of Net-Zero Energy Buildings, John Wiley & Sons, New Jersey, USA, 2015.
[23] ANSI/ASHRAE, *ASHRAE Handbook - Fundamentals*. American Society of Heating, Refrigerating and Air Conditioning Engineers: Atlanta, GA, USA, 2009.
[24] T. Frank, Climate change impacts on building heating and cooling energy demand in Switzerland, Energ. Buildings 37 (11) (2005) 1175–1185, https://doi.org/10.1016/j.enbuild.2005.06.019.
[25] M. Kolokotroni, X. Ren, M. Davies, A. Mavrogianni, London's urban heat Island: impact on current and future energy consumption in office buildings, Energ. Build. 47 (2012) 302–311, https://doi.org/10.1016/j.enbuild.2011.12.019.
[26] M. Cellura, F. Guarino, S. Longo, G. Tumminia, Climate change and the building sector: modelling and energy implications to an office building in southern Europe, Energy Sustain. Dev. 45 (2018) 46–65, https://doi.org/10.1016/j.esd.2018.05.001.
[27] A. Roetzel, A. Tsangrassoulis, Impact of climate change on comfort and energy performance in offices, Build. Environ. 57 (2012) 349–361, https://doi.org/10.1016/j.buildenv.2012.06. 002.
[28] A. Boyano, P. Hernandez, O. Wolf, Energy demands and potential savings in European office buildings: case studies based on EnergyPlus simulations, Energ. Build. 65 (2013) 19–28, https://doi.org/10.1016/j.enbuild.2013.05.039.
[29] E. Moreci, G. Ciulla, V. Lo Brano, Annual heating energy requirements of office buildings in a European climate, Sustain. Cities Soc. 20 (2016) 81–95, https://doi.org/10.1016/j.scs.2015.10.005.
[30] D. Sánchez-García, C. Rubio-Bellido, M. Tristancho, M. Marrero, A comparative study on energy demand through the adaptive thermal comfort approach considering climate change in office buildings of Spain, Build. Simul. 13 (1) (2020) 51–63, https://doi.org/10.1007/s12273-019-0560-2.
[31] H. Hooyberghs, S. Verbeke, D. Lauwaet, H. Costa, G. Floater, K. De Ridder, Influence of climate change on summer cooling costs and heat stress in urban office buildings, Clim. Change 144 (4) (2017) 721–735, https://doi.org/10.1007/s10584-017-2058-1.
[32] R.F. De Masi, A. Gigante, S. Ruggiero, G.P. Vanoli, Impact of weather data and climate change projections in the refurbishment design of residential buildings in cooling dominated climate, Appl. Energy 303 (2021), https://doi.org/10.1016/j.apenergy.2021.117584.
[33] F. Ascione, R.F. De Masi, A. Gigante, G.P. Vanoli, Resilience to the climate change of nearly zero energy-building designed according to the EPBD recast: Monitoring, calibrated energy models and perspective simulations of a Mediterranean nZEB living lab, Energ. Build. 262 (2022), https://doi.org/10.1016/j.enbuild.2022.112004.
[34] M. Kottek, J. Grieser, C. Beck, B. Rudolf, F. Rubel, World map of the Köppen-Geiger climate classification updated, Meteorol. Z. 15 (3) (2006) 259–263, https://doi.org/10.1127/0941-2948/2006/0130.
[35] R. Rahif et al., Impact of climate change on nearly zero-energy dwelling in temperate climate: time-integrated discomfort, HVAC energy performance, and GHG emissions, Build. Environ. 223 (2022), https://doi.org/10.1016/j.buildenv.2022.109397.
[36] ISO, *ISO 15927-2: Hygrothermal performance of buildings - Calculation and presentation of climatic data - Part 2: Hourly data for design cooling load*. International Standards Organization: Geneva, Switzerland, 2009.
[37] ISO, *ISO 7730: Ergonomics of the thermal environment - Analytical determination and interpretation of thermal comfort using calculation of the PMV and PPD indices and local thermal comfort criteria*. International Standards Organization: Geneva, Switzerland, 2004.
[38] W. Liping, W.N. Hien, Applying natural ventilation for thermal comfort in residential buildings in Singapore, Archit. Sci. Rev. 50 (3) (2007) 224–233, https://doi.org/10.3763/asre.2007.5028.
[39] ANSI/ASHRAE, *ASHRAE standard 55: Thermal environmental conditions for human occupancy*. American Society of Heating, Refrigerating and Air Conditioning Engineers: Atlanta, GA, USA, 2020.
[40] A.S. Silva, E. Ghisi, R. Lamberts, Performance evaluation of long-term thermal comfort indices in building simulation according to ASHRAE Standard 55, Build. Environ. 102 (2016) 95–115, https://doi.org/10.1016/j.buildenv.2016.03.004.
[41] D. Abd El-Raheim, A. Mohamed, M. Fatouh, H. Abou-Ziyan, Comfort and economic aspects of phase change materials integrated with heavy-structure buildings in hot climates, Appl. Therm. Eng. 213 (2022), https://doi.org/10.1016/j.applthermaleng.2022.118785.
[42] CIBSE, *CIBSE TM 52: The limits of thermal comfort: Avoiding overheating in European buildings*. Chartered Institution of Building Services Engineers: London, UK, 2015.
[43] T. Moore, I. Ridley, Y. Strengers, C. Maller, R. Horne, Dwelling performance and adaptive summer comfort in low-income Australian households, Build. Res. Inf. 45 (4) (2016) 443–456, https://doi.org/10.1080/09613218.2016.1139906.
[44] O. Dartevelle, G. van Moeseke, E. Mlecnik, S. Altomonte, Long-term evaluation of residential summer thermal comfort: measured vs. perceived thermal conditions in NZEB houses in Wallonia, Build. Environ. 190 (2021), https://doi.org/10.1016/j.buildenv.2020.107531.
[45] S. Salimi, E. Estrella Guillén, H. Samuelson, Exceedance Degree-Hours: a new method for assessing long-term thermal conditions, *Indoor Air* 31 (6) (2021) 2296–2311, https://doi.org/10.1111/ina.12855.
[46] ANSI/ASHRAE, *ASHRAE standard 169: Climatic data for building design standards*. American Society of Heating, Refrigerating and Air Conditioning Engineers Atlanta, GA, USA, 2013.
[47] G. Betti, F. Tartarini, C. Nguyen, S. Schiavon, "CBE Clima Tool: A free and open-source web application for climate analysis tailored to sustainable building design," V.0.7.3, 2022, doi: doi.org/10.48550/arxiv.2212.04609.
[48] InnoDez, "HVAC design - Sizing & design principles - 1," InnoDez Engineering, 2021. [online]. Available: www.innodez.com/hvac-design-sizing-design-principles/, Accessed on: Mar. 14, 2022.
[49] R. Rahif, D. Amaripadath, S. Attia, Review on time-integrated overheating evaluation methods for residential buildings in temperate climates of Europe, Energ. Build. 252 (2021), https://doi.org/10.1016/j.enbuild.2021.111463.
[50] M. Hamdy, S. Carlucci, P.J. Hoes, J.L.M. Hensen, The impact of climate change on the overheating risk in dwellings - A Dutch case study, Build. Environ. 122 (2017) 307–323, https://doi.org/10.1016/j.buildenv.2017.06.031.
[51] CEN, *EN 16798-1: Energy performance of buildings - Ventilation for buildings - Indoor environmental input parameters for design and assessment of energy performance of buildings addressing indoor air quality, thermal environment, lighting and acoustics*. European Committee for Standardization: Brussels, Belgium, 2019.
[52] ISO, *ISO 17772-1: Energy performance of buildings - Indoor environmental quality. Part 1: Indoor environmental input parameters for the design and assessment of energy performance in buildings*. International Standards Organization: Geneva, Switzerland, 2017.
[53] CIBSE, *CIBSE Guide A: Environmental design*. Chartered Institution of Building Services Engineers: London, UK, 2015.
[54] R. Rahif, M. Hamdy, S. Homaei, C. Zhang, P. Holzer, S. Attia, Simulation-based framework to evaluate resistivity of cooling strategies in buildings against overheating impact of climate change, Build. Environ. 208 (2022), https://doi.org/10.1016/j.buildenv.2021.108599.
[55] M. Carlier, "nearly Zero-Energy Building definitions in selected countries," Master Thesis, Ghent University, Ghent, Belgium, Jul. 2016. [Online]. Available: www.libstore.ugent.be/fulltxt/RUG01/002/301/ 108/RUG01-002301108_2016_0001_AC.pdf.
[56] IBGE, "Performance Energétique des Bâtiments: Guide des exigences et des procédures de la 960 réglementation Travaux PEB en Région de Bruxelles Capitale," Brussels, Belgium, 2017.
[57] Encon, "Calculation of CO2," Encon. [online]. Available: www.encon.be/en/calculation-co2, Accessed on: Jul. 11, 2022.
[58] V. Pérez-Andreu, C. Aparicio-Fernández, A. Martínez-Ibernón, J.L. Vivancos, Impact of climate change on heating and cooling energy demand in a residential building in a Mediterranean climate, Energy 165 (2018) 63–74, https://doi.org/10.1016/j.energy.2018.09.015.
[59] C. Kittel, "Present and future sensitivity of the Antarctic surface mass balance to oceanic and atmospheric forcings: insights with the regional climate model MAR," University of Liege, Belgium, 2021. [Online]. Available: http://hdl.handle.net/2268/258491.
[60] C. Wyard, C. Scholzen, S. Doutreloup, É. Hallot, X. Fettweis, Future evolution of the hydroclimatic conditions favouring floods in the south-east of Belgium by 2100 using a regional climate model, Int. J. Climatol. 41 (1) (2021) 647–662, https://doi.org/10.1002/joc.6642.
[61] S. Doutreloup et al., Sensitivity to convective schemes on precipitation simulated by the regional climate model MAR over Belgium (1987–2017), Atmos. 10 (1) (2019) 34, https://doi.org/10.3390/atmos10010034.
[62] A. Moazami, V.M. Nik, S. Carlucci, S. Geving, Impacts of future weather data typology on building energy performance - Investigating long-term patterns of climate change and extreme weather conditions, Appl. Energy 238 (2019) 696–720, https://doi.org/10.1016/j.apenergy.2019.01.085.

[63] K. De Ridder, H. Gallée, Land surface-induced regional climate change in southern Israel, J. Appl. Meteorol. Climatol. 37 (11) (1998) 1470–1485, https://doi.org/10.1175/1520-0450(1998)037<1470:LSIRCC>2.0.CO;2.
[64] H. Hersbach et al., The ERA5 global reanalysis, Q. J. R. Meteorolog. Soc. 146 (730) (2020) 1999–2049, https://doi.org/10.1002/qj.3803.
[65] V. Eyring et al., Overview of the coupled model intercomparison project phase 6 (CMIP6) experimental design and organization, Geosci. Model Dev. 9 (5) (2016) 1937–1958, https://doi.org/10.5194/gmd-9-1937-2016.
[66] S. Doutreloup et al., Historical and future weather data for dynamic building simulations in Belgium using the regional climate model MAR: typical and extreme meteorological year and heatwaves, Earth Syst. Sci. Data 14 (2022) 3039–3051, https://doi.org/10.5194/essd-14-3039-2022.
[67] V. Masson-Delmotte et al., "Climate Change 2021: The Physical Science - Basis Contribution of Working Group I to the Sixth Assessment Report of the Intergovernmental Panel on Climate Change," 2021.
[68] K. Riahi et al., The Shared Socioeconomic Pathways and their energy, land use, and greenhouse gas emissions implications: an overview, Glob. Environ. Chang. 42 (2017) 153–168, https://doi.org/10.1016/j.gloenvcha.2016.05.009.
[69] ISO, *ISO 15927-4: Hygrothermal performance of buildings - Calculation and presentation of climatic data - Part 4: Hourly data for assessing the annual energy use for heating and cooling.* International Standards Organization: Geneva, Switzerland, 2005.
[70] Performance Énergétique des Bâtiments, "La performance énergétique des bâtiments - La PEB, une réglementation à 3 volets," Environnement Brussels, Belgium. [Online]. Avaiable: www.environn ement.brussels/thematiques/batiment-et-energie/obligations/la-performance-energetique-des-batiments-peb, Accessed on: Feb. 25, 2022.
[71] M. Hamdy, K. Sirén, S. Attia, Impact of financial assumptions on the cost optimality towards nearly zero energy buildings – a case study, Energ. Build. 153 (2017) 421–438, https://doi.org/10.1016/j.enbuild.2017.08.018.
[72] S. Attia, N. Shadmanfar, F. Ricci, Developing two benchmark models for nearly zero energy schools, Appl. Energy 263 (2020), https://doi.org/10.1016/j.apenergy.2020.114614.
[73] CEN, *EN 13829: Thermal performance of buildings - Determination of air permeability of buildings - Fan pressurization method*. European Committee for Standardization: Brussels, Belgium, 2001.
[74] CEN, *EN 16798-2: Energy performance of buildings - Ventilation for buildings - Part 2: Interpretation of the requirements in EN 16798-1 - Indoor environmental input parameters for design and assessment of energy performance of buildings addressing indoor air quality, thermal environment, lighting and acoustics*. European Committee for Standardization: Brussels, Belgium, 2019.
[75] D. Amaripadath, M. Velickovic, S. Attia, Performance evaluation of a nearly zero-energy office building in temperate oceanic climate based on field measurements, *Energies* 15 (18) (2022), https://doi.org/10.3390/en15186755.
[76] R. Fassbender, "What is energy model calibration? pt 1," Energy Models. [online]. Available: www.energy-models.com/blog/what-energy-model-calibration-pt-1, Accessed on: Mar. 14, 2022.
[77] A. Chong, Y. Gu, H. Jia, Calibrating building energy simulation models: a review of the basics to guide future work, Energ. Build. 253 (2021), https://doi.org/10.1016/j.enbuild.2021.111533.
[78] ANSI/ASHRAE, *ASHRAE Guideline 14: Measurement of energy, demand, and water savings*. American Society of Heating, Refrigerating and Air Conditioning Engineers: Atlanta, GA, USA, 2014.
[79] G.R. Ruiz, C.F. Bandera, Validation of calibrated energy models: common errors, Energies 10 (10) (2017) Oct, https://doi.org/10.3390/en10101587.
[80] J. Shinoda, O.B. Kazanci, S. Tanabe, B.W. Olesen, A review of the surface heat transfer coefficients of radiant heating and cooling systems, Build. Environ. 159 (2019), https://doi.org/10.1016/j.buildenv.2019.05.034.
[81] O.B. Kazanci, "Low temperature heating and high temperature cooling in buildings," Ph.D. Thesis, Technical University of Denmark, Kongens Lyngby, Denmark, 2016. [Online]. Available: www.backend.orbit.dtu.dk/ws/portalfiles/portal/126945749/Thesis_til_orbit.pdf.
[82] D.I. Dragos, O.B. Kazanci, B.W. Olesen, An experimental study of the active cooling performance of a novel radiant ceiling panel containing phase change material (PCM), Energ. Build. 243 (2021), https://doi.org/10.1016/j.enbuild.2021.110981.
[83] J. Babiak, B.W. Olesen, D. Petras, "Low temperature heating and high temperature cooling," 2nd ed., Technical Task Force 3, REHVA: Federation of European Heating, Ventilation and Air Conditioning Associations, Brussels, Belgium.
[84] T. Dwyer, "Module 51: Air source VRF systems for flexible room heating and cooling, heat recovery and hydronic heating," *CIBSE Journal*, 2013. [online]. Available: www.cibsejournal.com/cpd/modules/2013-04/, Accessed on: Mar. 22, 2022.
[85] M. Coley, "What is a VRF system? Top myths and facts about VRF explained," Ferguson Enterprises, 2018. [online]. Available: www.ferguson.com/content/trade-talk/tricks-of-the-trade/what-is-a-vrf-system, Accessed on: Mar. 16, 2022.
[86] K. Taylor, "EU paves way for renewable and low-carbon gases to replace fossil fuel," Euractiv, Dec. 2021. [online]. Available: www.euractiv.com/section/energy/news/eu-paves-way-for-renewable-and-low-carbon-gases-to-replace-fossil-fuel/, Accessed on: Mar. 23, 2022.
[87] M. Tobias, "Heating and cooling system configurations for commercial buildings," Nearby Engineers, 2021. [online]. Available: www.ny-engineers.com/blog/heating-and-cooling-system-configurations-for-commercial-buildings, Accessed on: Mar. 16, 2022.
[88] W. Luan, X. Li, Rapid urbanization and its driving mechanism in the Pan-Third Pole region, Sci. Total Environ. 750 (2021), https://doi.org/10.1016/j.scitotenv.2020.141270.
[89] M. Luo et al., The dynamics of thermal comfort expectations: the problem, challenge and implication, Build. Environ. 95 (2016) 322–329, https://doi.org/10.1016/j.buildenv.2015.07.015.
[90] United Nations, "World population prospects: The 2017 revision," *United Nations Department of Economic and Social Affairs*, United Nations, New York, USA, 2017.
[91] EEA, "EU renewable electricity has reduced environmental pressures; Targeted actions help further reduce impacts: Briefing," *European Environment Agency*, Copenhagen, Denmark, 2021. [Online]. Available: www.eea.europa.eu/themes/energy/renewable-energy/eu-renewable-electricity-has-reduced. Accessed: Jul. 19, 2022.
[92] Y. Lou, Y. Ye, Y. Yang, W. Zuo, Long-term carbon emission reduction potential of building retrofits with dynamically changing electricity emission factors, Build. Environ. 210 (2022).
[93] S. Attia, et al. "Framework to evaluate the resilience of different cooling technologies." Liege, Belgium: Sustainable Building Design Lab, 2021, doi:10.13140/RG.2.2.33998.59208.
[94] DGBG, "SAPP ceiling," *Dutch Green Building Guide*. [Online]. Available: www.dgbg.nl/product/263. Accessed: Jul. 20, 2022.
[95] Interalu, "Discover SAPPceiling," *Interalu Smart Ceilings*. [Online]. Available: www.interalu.eu/en/kennis/discover-sappceiling. Accessed: Jul. 20, 2022.
[96] D. Amaripadath, R. Rahif, M. Velickovic, S. Attia, A systematic review on role of humidity as an indoor thermal comfort parameter in humid climates, J. Build. Eng. 68 (2023), https://doi.org/10.1016/j.jobe.2023.106039.
[97] R. Rahif, D. Amaripadath, and S. Attia, "Review on Overheating Evaluation Methods in National Building Codes in Western Europe", CLIMA, May 2022, doi: doi.org/10.34641/clima.2022.357.
[98] EC, "Delivering the European Green Deal," *European Commission*, Brussels, Belgium, 2022. [Online]. Available: ec.europa.eu/info/strategy/priorities-2019-2024/european-green-deal/delivering-european-green-deal_en. Accessed: Jul. 19, 2022.
[99] C. Zhang et al., Resilient cooling strategies – A critical review and qualitative assessment, Energ. Build. 251 (2021), https://doi.org/10.1016/j.enbuild.2021.111312.
[100] J. Żuławińska, "Wet bulb calculator," Omni Calculator, 2022. [online]. Available: www.omnicalculator.com/physics/wet-bulb, Accessed on: Mar. 17, 2022.
[101] D.J. Vecellio, S.T. Wolf, R.M. Cottle, W.L. Kenney, Evaluating the 35°C wet-bulb temperature adaptability threshold for young, healthy subjects (PSU HEAT Project), J. Appl. Physiol. 132 (2) (2022) 340–345, https://doi.org/10.1152/japplphysiol.00738.2021.
[102] Legal Information Institute, "10 CFR § 431.97 - Energy efficiency standards and their compliance dates," Cornell Law School, NY, USA. [Online]. Available: https://www.law.cornell.edu/cfr/text/10/431.97#fn1_tbl2. Accessed on: Dec. 12, 2022.
[103] HVAC HESS, "Heat Pump and Heat Recovery Technologies," Department of Climate Change, Energy, the Environment and Water, Australia, 2013. [Online]. Available: https://www.environment.gov.au/system/files/energy/files/hvac-factsheet-heat-pump-tech.pdf. Accessed on: Dec. 12, 2022.
[104] DesignBuilder, "VRF Outdoor Unit," DesignBuilder Resources, Gloucs, UK. [Online]. Available: www.designbuilder.co.uk/helpv7.0/Content/VRFOutdoorUnit.htm, Accessed on: Jul. 20, 2022.